



universität  
wien

# DIPLOMARBEIT

Titel der Diplomarbeit

**„Mechanisms of Oligodendrocyte Precursor Cell Differentiation“**

1 von 1

Verfasserin

Tamara Weiss, BSc

angestrebter akademischer Grad

Magistra der Naturwissenschaften (Mag.rer.nat.)

Wien, 2011

Studienkennzahl lt. Studienblatt:

A 490

Studienrichtung lt. Studienblatt:

Molekulare Biologie

Betreuer:

Professor Friedrich Propst

## Acknowledgement

First of all I would like to thank my supervisor Dr Mark Kotter for offering me the opportunity to perform the practical part of my diploma thesis in his lab at the Anne McLaren Laboratory for Regenerative Medicine, University of Cambridge. In his group and the institute I found various people I want to thank like Yasir Syed who diligently introduced me into numerous new techniques, Matthias Hofer for his everyday support and guidance, Dr Sasha Mendjan for his help in methods optimisation as well as all others colleagues which I experienced outstanding kind and helpful during my whole stay.

Last but not least I have to mention that without funding my stay in Cambridge would not have been affordable and therefore, I thank the University of Vienna for its 'Förderstipendium der Universität Wien', the province of lower Austria for its 'Niederösterreich Top-Stipendium Ausland' and my family that supported me all along the way.



universität  
wien





## Abstract (English)

*Oligodendrocytes* are the myelin-producing cells in the central nervous system (CNS) and constitute the pendant to the myelinating *Schwann cells* in the peripheral nervous system (PNS). Whilst myelin formation for axonal insulation to ensure rapid impulse propagation, oligodendrocytes have gained a prominent role in the maintenance of axonal integrity. Therefore, oligodendrocytes are detached from the former passive role as a supporter cell of neurons to an indispensable, active companion to assure neuronal preservation. Further, oligodendrocytes are the target in developmental defects like Pelizaeus-Merzbacher disease and devastating degenerative diseases like Multiple Sclerosis (MS). To understand the presumably failure of re-myelination in chronic MS lesions and for establishing new therapies to avoid de-myelination or enhance re-myelination, the efficient research in *oligodendrocyte precursor cell* (OPC) differentiation is constitutive. The mechanisms of myelination are thought to be related to those of re-myelination. Thus, detailed knowledge about the cellular and molecular processes that underlie myelination is necessary to provide insights into myelin regeneration. As recent experiments regarding the impact of Eph-receptors and Ephrins on oligodendrocyte differentiation suggest a receptor mediated differentiation block, new studies are needed to explore those pathways of OPC differentiation. Thus, this study focussed on experiments that investigate the mechanisms of oligodendrocyte precursor cell differentiation through analyzing of Eph-receptor mediated pathways as well as brain samples from EphrinB3 knockout mice compared to controls. In addition, established primary oligodendrocyte cell differentiation experiments were tried to be reproduced by the oligodendrocyte cell lines OLN-93 and OLI-Neu for both the reduction of animal sacrifices and a faster realization of experiments. The results revealed the OLN-93 and OLI-Neu cell lines to be not suitable for the simulation of OPC differentiation *in vitro* and to probably represent oligodendroglial cells conserved in earlier stages of development. However, the most important finding in this study indicated that EphrinB3 knock out in day 2 mice promotes premature myelination of axons compared to controls. As EphrinB3 was shown to act inhibitory on OPC differentiation *in vitro*, this result strengthens EphrinB3 to be a crucial element in oligodendrocyte development.

## Abstract (German)

*Oligodendrozyten* sind die Myelin produzierenden Zellen des Zentralen Nervensystems und stellen das Gegenstück zu den myelinierenden *Schwann-Zellen* des Peripheren Nervensystems dar. Neben der Produktion von Myelin für die Isolation von Axonen um die schnelle Weiterleitung von Nervenimpulsen zu gewährleisten, haben die Oligodendrozyten in den letzten Jahren immer größere Bedeutung für die Bewahrung der Integrität von Axonen erlangt. Diese Loslösung der bis dahin passiv gesehenen Aufgabe der Neuronenunterstützung hat die Oligodendrozyten zu aktiven Begleitern der Neuronen erhoben, die sich unverzichtbar für deren Erhalt herausgestellt haben. Weiters hat sich gezeigt, dass Oligodendrozyten das Ziel von neurodegenerativen Krankheiten wie Pelizaeus-Merzbacher oder Multipler Sklerose (MS) sind und beispielsweise chronische MS Läsionen auf Fehler in der Re-Myelinierung von Axonen hinweisen. Neue Therapien zur Vermeidung von De-Myelinierung oder zur Wiederherstellung von Myelin werden dringend benötigt, aber leider weiß man noch zu wenig über den Ablauf und Fehler von Myelinierungsvorgängen. Effiziente Forschung und neue Strategien sind demnach unerlässlich um detailreiches Wissen über die zellulären und molekularen Prozesse anzureichern, die der Differenzierung von Oligodendrozyten zugrunde liegen da sie sehr wahrscheinlich jenen der Re-Myelinierung ähneln. Kürzlich erbrachte Experimente, welche die Auswirkung von Eph-Rezeptoren und Ephrinen auf Oligodendrozyten untersucht haben, konnten eine rezeptorbasierende Blockierung der Differenzierung nachweisen. Da die Signalwege der Differenzierung von Oligodendrocyten-Vorläuferzellen (OPCs) bis hin zu myelinierenden Oligodendrozyten kaum bekannt sind, beschäftigt sich diese Studie mit Experimenten, welche die Mechanismen der Differenzierung von OPCs durch Eph-Rezeptoren vermittelte Signalwege und Gehirnproben von EphrinB3 Knock-Out Mäusen im Vergleich zu Kontrollen analysieren. Außerdem wurde versucht, etablierte Primär-Zellkultur Experimente zur Oligodendrozyten Differenzierung mit Zelllinien zu reproduzieren um sowohl die Anzahl der benötigten Tiere zu reduzieren, als auch eine schnellere Umsetzung dieser Experimente realisieren zu können. Die Ergebnisse haben jedoch gezeigt, dass die OLN-93 und OLI-Neu OPC Zelllinien dafür nicht geeignet sind und wahrscheinlich Frühstadien von Oligodendrozyten repräsentieren, die in dieser Entwicklungsphase konserviert sind. Von großer Bedeutung war jedoch ein Ergebnis, welches auf eine verfrühte Myelinierung von Axonen in zwei Tage alten Hirnen von EphrinB3 Knock-Out Mäusen hindeutet. Da sich EphrinB3 in *in vitro* Versuchen inhibierend auf die Oligodendrozyt-Vorläuferzellen Differenzierung auswirkt, unterstreicht dieses Ergebnis die wichtige Rolle von EphrinB3 in der Oligodendrozyten Entwicklung.

## TABLE OF CONTENTS

<b>1. INTRODUCTION</b>	<b>9</b>
1.1 THE CENTRAL NERVOUS SYSTEM (CNS)	9
1.2 OLIGODENDROCYTE PRECURSOR CELLS (OPCs)	9
1.2.1 OLIGODENDROCYTE PRECURSORS IN THE SPINAL CORD	9
1.2.2 EARLY OLIGODENDROCYTE LINEAGE MARKERS	10
1.2.3 OLIGODENDROCYTE PRECURSORS IN THE FORE BRAIN	10
1.3 MATURATION OF OLIGODENDROCYTES	11
1.4 THE MYELINATING OLIGODENDROCYTE	11
1.5 DEMYELINATION AND RE-MYELINATION IN THE CNS	12
1.6 RE-MYELINATION FAILURE AND DISEASE	13
1.7 EPHRINS & EPH-RECEPTORS	15
<b>2. PROJECT OVERVIEW</b>	<b>17</b>
2.1 ANALYSING OF PRIMARY OPCs VERSUS OPC CELL LINES	17
2.2 EM ANALYSIS OF MYELIN ABNORMALITIES IN EPHRINB3 KNOCK-OUT MICE	20
2.3 EPHRINB3 AND ITS RECEPTORS	21
<b>3. METHODS</b>	<b>23</b>
3.1 PREPARATION OF MIXED GLIAL CELLS (MGCs)	23
3.2 PURIFICATION OF OPCs (SHAKE-OFF)	23
3.3 PREPARATION OF MYELIN MEMBRANE SUBSTRATES AND MYELIN PROTEIN EXTRACTS	24
3.4 DETERMINATION OF PROTEIN CONCENTRATION (BCA)	25
3.5 IMMUNOPRECIPITATION	25
3.5.1 IMMUNOPRECIPITATION OVERVIEW	26
3.6 SDS-PAGE	27
3.7 WESTERN-BLOT	27
3.8 EMBEDDING OF BRAIN TISSUE	28
3.9 PREPARING OF EM-SLICES	29
3.10 IMMUNOCYTOCHEMISTRY	29
3.10.1 FIXATION OF CELLS	29
3.10.2 BLOCKING/PERMEABILISATION STEP	29
3.10.3 STAINING	30
3.11 DIFFERENTIATION OF OLN-93 AND OLI-NEU CELL LINES	30
3.12 OTHERS	31
3.12.1 HARVESTING OF OLN-93 & OLI-NEU CELL LINES FROM FLASKS	31
3.12.2 THAWING OF OLN-93 & OLI-NEU CELL LINES	31
3.12.3 FREEZING OF OLN-93 & OLI-NEU CELL LINES	32
3.12.4 CELL NUMBER CALCULATION	32
3.12.5 CLUSTERING OF EPHRINB3	32

---

## **4. MATERIALS** **34**

---

<b>4.1 PRIMARY OPCs</b>	<b>34</b>
<b>4.2 OPC CELL LINES</b>	<b>34</b>
4.2.1 OLI-NEU	34
4.2.2 OLN-93	34
<b>4.3 EPHRINB3 KNOCK-OUT MICE</b>	<b>34</b>
<b>4.4 CELL CULTURE MEDIA</b>	<b>35</b>
4.4.1 OLI-NEU CULTIVATION MEDIA	35
4.4.2 OLI-NEU DIFFERENTIATION MEDIA	35
4.4.3 OLN-93 CULTIVATION MEDIA	35
4.4.4 OLN-93 DIFFERENTIATION MEDIA	35
4.4.5 MEM	35
4.4.6 SATOS MEDIA	35
4.4.7 OPC DIFFERENTIATION MEDIA	35
<b>4.5 BUFFERS</b>	<b>36</b>
<b>4.6 SOLUTIONS</b>	<b>37</b>
<b>4.7 CHEMICALS</b>	<b>39</b>

---

## **5. RESULTS** **42**

---

<b>5.1 PRIMARY OPCs vs. OPC CELL LINES</b>	<b>42</b>
5.1.1 ANALYSIS OF PRIMARY OPC MORPHOLOGY AND DIFFERENTIATION POTENTIAL.	42
5.1.2 ANALYSIS OF OPC CELL LINE MORPHOLOGY	43
5.1.2.1 OLI-NEU MORPHOLOGY IN DIVERSE MEDIA CONDITIONS	44
5.1.2.2 OLN-93 MORPHOLOGY IN DIVERSE MEDIA CONDITIONS	45
5.1.3 ANALYSIS OF MORPHOLOGY AND DIFFERENTIATION POTENTIAL WITH IMMUNOCYTOCHEMISTRY MARKERS	45
5.1.3.1 OLI-NEU CELL LINE DIFFERENTIATION POTENTIAL	46
5.1.3.2 OLN-93 CELL LINE DIFFERENTIATION POTENTIAL	47
5.1.3.3 MORPHOLOGICAL DIFFERENCES BETWEEN PRIMARY OPCs AND CELL LINE CELLS	48
5.1.3.4 MORPHOLOGICAL STAGES OF OLI-NEU AND PRIMARY OPC PROCESS FORMATION	48
5.1.4 ANALYSIS OF THE INHIBITORY POTENTIAL OF MPE AND EPHRINB3	50
5.1.4.3 OPCs ON PLL	50
5.1.4.4 OPCs ON MPE	50
5.1.4.5 OLI-NEU CELLS ON PLL	50
5.1.4.4 OLI-NEU CELLS ON MPE	50
5.1.4.5 OLN-93 CELLS ON MPE	51
5.1.4.6 REACTION OF OPCs ON EPHRINB3	52
5.1.5 IMMUNOCYTOSTAINING RESULTS OVERVIEW	52
<b>5.2 POTENTIAL OPC-ASTROCYTE SWITCH</b>	<b>53</b>
<b>5.3 EM ANALYSIS OF EPHRINB3 KO MICE</b>	<b>54</b>
5.3.1 ANALYSING OF G-RATIOS	54
5.3.2 DIFFERENCES IN MYELINATION	54
5.3.3 MYELIN ABNORMALITIES	57
<b>5.4 ANALYSING OF EPHRINB3 AND ITS RECEPTORS</b>	<b>58</b>
5.4.1 IP AND PHOSPHORYLATION ANALYSIS OF EPHRIN RECEPTORS	58
5.4.2 IP OF EPH RECEPTORS	60
5.4.3 IP OF EPHRINB3 OUT OF MPE	60
5.4.4 IP OF EPHRINB3 OUT OF PRIMARY OLIGODENDROCYTE LYSATES	62

---

<b>6. DISCUSSION</b>	<b>64</b>
<b>6.1 PRIMARY OPCs VERSUS CELL LINES</b>	<b>64</b>
6.1.1 PRIMARY OPC EXPERIMENTS	64
6.1.2 ANALYSIS OF OPC CELL LINE OLN-93 DISPLAYED THEM TO BE NOT	64
6.1.3 OLI-NEU CELLS	65
6.1.4 SUMMARY	65
<b>6.2 POTENTIAL OLIGODENDROCYTE-ASTROCYTE SWITCH <i>IN VITRO</i> WITH 10% FCS</b>	<b>66</b>
<b>6.3 DAY 2 EPHRINB3 KO MICE SHOWED A PREMATURE BEGINNING OF ACTIVE MYELINATION</b>	<b>66</b>
<b>6.4 EPHRINB3 AND ITS RECEPTORS EPH B1, B2, B3 &amp; A4</b>	<b>67</b>
6.4.1 EPH RECEPTORS B1, B2, B3 & A4 WERE PROBABLY PRECIPITATED WITH CELL MEMBRANE DEBRIS	67
6.4.2 EPHRINB3 PROBABLY FAILED	67
<b>7. REFERENCES</b>	<b>68</b>
<b>8. APPENDIX</b>	<b>73</b>
<b>8.1 CURRICULUM VITAE</b>	<b>73</b>

# Introduction

The CNS

Oligodendrocyte Precursor Cells (OPCs)

OPC lineage markers

Maturation of OPCs

Demyelination & Re-myelination

Re-myelination failure and disease

Ephrins and Eph receptors

## 1. Introduction

### 1.1 The central nervous system (CNS)

The CNS is primarily constituted by *neuronal* and *glial cells*. While the different types of neurons are needed for the propagation of nerve impulses, the glial cells have shown to be necessary for the correct development, support and protection of neuronal cells. Formerly known as the 'nervenkitt' (nerve glue)<sup>1</sup> the role of glia (glia = greek for glue) changed in both function and importance and today, glial cells represent active partners of neurons to ensure their integrity and regeneration.<sup>2</sup> Thereby, two types of glia are divided: macroglia and microglia. While macroglia arise from the neuroectoderm and form astrocytes, ependymal cells and *oligodendrocytes*, microglia develop from the mesoderm into the resident macrophages.

### 1.2 Oligodendrocyte precursor cells (OPCs)

Oligodendrocytes are the myelin forming cells of the CNS and mature from so called *oligodendrocyte precursor cells* (OPCs) that are generated from pluripotent neuroepithelial cells within the spinal cord and ventricles of the brain. During development, OPCs migrate through the spinal cord and the brain grey and white matter to their final destinations where they differentiate into myelin forming cells.<sup>3</sup> When OPCs are isolated from P0-P2 rat cortices or P7 rat optic nerve, they can be differentiated into astrocytes or oligodendrocytes dependent on the used serum percentage.<sup>4</sup> However, in adult brains they arise from neuronal stem cell populations that are resident in the subventricular zone (SVZ), the hippocampus or in the spinal cord<sup>5,6</sup>.

Most valuable about isolated OPCs is indeed that their maturation from the oligodendrocyte precursor cell until the myelinating oligodendrocyte seems to follow the same stages as *in vivo* (compare figure1). This suggests OPCs to have an intrinsic differentiation capacity<sup>7</sup> and thus, oligodendrocyte development can be studied *in vitro* even without neurons.<sup>4,8</sup> However, the co-culture of OPCs with neurons increases the myelin expression.<sup>9</sup>

#### 1.2.1 Oligodendrocyte Precursors in the spinal cord

Oligodendrogenesis was first thought to be restricted to the ventral *ventricular zone* (VZ) of the embryonic neural tube<sup>10</sup>, specifically to the *neuroepithelial domain* (pMN), but there is also a minor population (~15%) that arises from dorsal parts of the VZ.<sup>11,12</sup> The pMN creates motor neurons in the first place and changes to oligodendrocyte precursor cell production about embryonic day (E)12.5, generation of dorsal OPCs follows about E15.<sup>13</sup>

### 1.2.2 Early oligodendrocyte lineage markers

In the developing vertebral neural tube the cell fate is dependent on the concentration of inductive and repressive signals. In the ventral midline, the glycoprotein *Sonic Hedgehog (SHH)* is secreted from the notochord and floor plate and co-ordinately regulates *Olig2/Olig1* gene expression in the pMN. Thereby, SHH activates the transcription factor *Nkx6.2* that in turn induces the formation of basic helix-loop-helix transcription factors *OLIG2 and OLIG1*<sup>14</sup>. Whereas *OLIG1* promotes OPC development and is necessary for maturation and myelin regeneration<sup>15</sup>, *OLIG2* is essential to induce motor neuron and oligodendrocyte specification in the neuroepithelia and is expressed during the whole oligodendrocyte development.<sup>16</sup> Further, *Olig2* gene expression is thought to be the first marker of spinal cord progenitor cells that develop into oligodendrocyte precursors.<sup>17</sup> Other established lineage markers of ventrally derived spinal cord OPCs are *NG2*<sup>18</sup>, *SOX10*<sup>19,20</sup>, platelet-derived growth factor receptor (*PDGFRα*)<sup>21</sup> and *nkx2.2*<sup>22</sup>. However, dorsally derived OPCs express those markers as well but very likely through hedgehog-independent pathways.<sup>12,25</sup>

### 1.2.3 Oligodendrocyte Precursors in the fore brain

Parts of the embryonic VZ in the forebrain produce OPCs as well but compared to the spinal cord at different times. However, they first appear at E12.5 from neuroepithelial cells of the *medial ganglionic eminence (MGE)*, situated in the ventral part of the telencephalon. They start migrating into the developing forebrain and at E18 only ventral derived OPCs are found in the cortex. This first wave of OPCs is then followed by a second one, originated from the *lateral and/or caudal ganglionic eminence/s (LGE/CGE)*. At least, parts of the neuroepithelium in the cortex itself produce a third wave of OPCs. These different OPC populations, all with a region specific expression of transcription factors, now mix and compete with one another for territory in the cortex. This would indicate specialized oligodendrocyte subtypes but there seem to be no significant differences as both ventral and dorsal derived forebrain OPCs are able to take over the others place when eliminated. Interestingly, the earliest, most ventral, MGE-derived OPC population progeny disappear upon postnatal life. After birth until adulthood, the *subventricular zone (SVZ)*, the hippocampus and some spinal cord regions remains active in generating new oligodendrocyte precursor cells.<sup>6</sup> As the SVZ is derived mainly from the embryonic LGE and lateral cortex, with no contribution from more ventral regions, any evidence of MGE-derived OPCs is erased in the adult brain.<sup>26</sup> SHH is suggested to have a similar role in oligodendrocyte development in the telencephalon like in the spinal cord.<sup>27</sup>



### 1.3 Maturation of oligodendrocytes

During the whole developmental process, the survival, maturation and differentiation of OPCs is regulated by growth factors, chemokines, soluble and cell mediated signals from neighbouring cells (neurons, astrocytes, ...) and the extracellular matrix. Maturation of oligodendrocytes is accompanied by changes in shape and expression of specific cell surface proteins. Some antigens are lost and new ones acquired so that they can function as lineage markers to identify the stage of oligodendrocyte differentiation.

In early development, the oligodendrocyte progenitor cells have shown to be NG2 & PDGFR $\alpha$  positive<sup>18,28,29</sup> and migrate throughout the CNS. They are still able to proliferate but this ability is dependent on PDGFR $\alpha$  expression. When the OPCs settle along the fiber tracts of the future white matter (E16), they start to express the marker O4 (O-antigens are sulfatides)<sup>30</sup> and transform into *pre-oligodendrocytes* that results in becoming less motile as they lose their mitotic response to PDGFR $\alpha$ .<sup>31,32,33</sup> By reaching their final target, the appearance of galactocerebroside (GalC)<sup>34</sup> characterizes the *immature oligodendrocyte*. Finally, the expression of the myelin proteins as *myelin basic protein* (MBP) along with *myelin associated glycoprotein* (MAG) followed by *proteolipid-protein* (PLP)<sup>35</sup> indicates the *mature (non-myelinating) oligodendrocyte* immediately before myelin formation. Important for terminal differentiation is the transcription factor Sox10 as it can directly induce expression of myelin genes.<sup>36</sup>

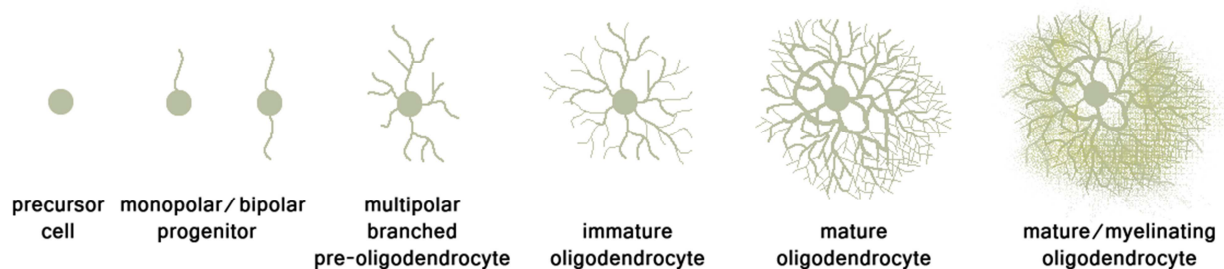
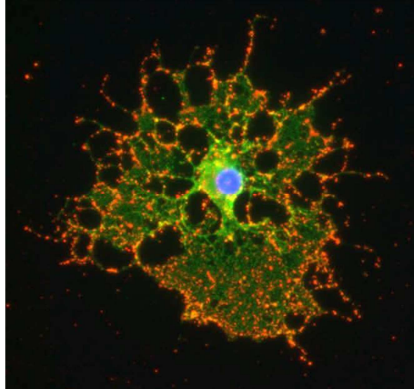


Figure 1 | Stages of oligodendrocyte differentiation.

### 1.4 The myelinating oligodendrocyte

The *myelinating oligodendrocyte* can form several myelin sheets, also called myelin internodes, to enwrap multiple segments of about 10 to 15 different neurons. For myelin sheets production several enzymes of the lipid metabolism have to be activated, the transcription factors Nkx2.2, Nkx6.1, Nkx6.2 are expressed<sup>37</sup> as well as proteins that are necessary for transport and synthesis of myelin mRNA or proteins.

Myelin itself is a lipid rich, multilamellar membrane, spirally wrapped around axon fibres to ensure their electrical insulation. Its segmental structure allows the fast and saltatory conduction of nerve



impulses as action potentials can only occur at un-myelinated regions between those segments, the *Nodes of Ranvier*. The importance of myelin can be shown by its loss in several neurological diseases such as multiple sclerosis in the CNS.

**Figure 2** | A myelinating oligodendrocyte at d4 after in vitro differentiation from an isolated primary OPC culture. The immunocytochemical staining shows antibodies against the oligodendrocyte marker O4 in red and against MBP (myelin sheet) in green.

### 1.5 Demyelination and Re-myelination in the CNS

Under normal conditions, the turnover of myelin is very slow.<sup>38</sup> The loss of myelin sheets through the direct insult or death of Oligodendrocytes is called *de-myelination* followed by neuronal conduction block. The default response to de-myelination is regeneration or the replacement through new Oligodendrocytes to restore neuronal integrity as the neuron itself is still alive. This spontaneous, regenerative phenomenon of *re-myelination* stands in contrast to the poor regeneration after neuronal injuries.<sup>39, 40</sup>

Two major events are necessary for re-myelination, first, the recruitment (activation, proliferation and migration) of OPCs from widespread populations in the CNS<sup>41,42</sup> or from the adult SVZ<sup>43,44</sup> to the place of lesion and second, the differentiation into a myelinating Oligodendrocyte to restore saltatory conduction.<sup>45</sup> However, in contrast to the myelin sheets that are acquired during development, in re-myelinated areas the normal relationship between axon and myelin sheet is never regained<sup>46</sup> as both the thickness and size of newly produced myelin is decreased.<sup>47,48</sup> The ratio of the inner axonal diameter to the total outer diameter called the *g-ratio*. Therefore, re-myelinated areas can be identified by abnormally thin myelin sheaths ( $> g$  ratio) but is only obvious at axons with a large diameter.<sup>49,50</sup>

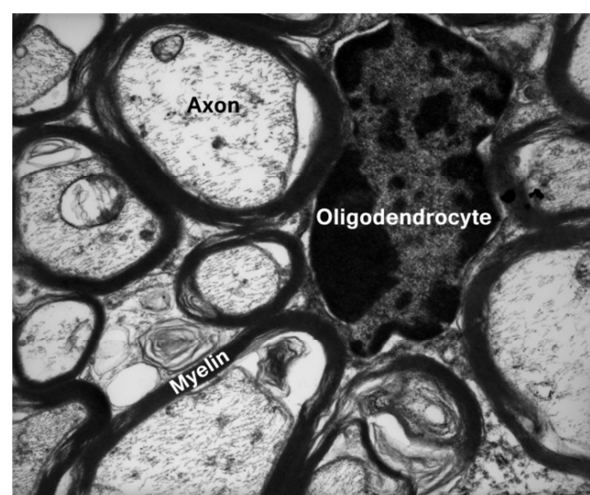


**Figure 3** | EM image of an oligodendrocyte surrounded by myelinated axons.

## 1.6 Re-myelination failure and disease

De-myelination in the CNS is caused by two major events, genetic abnormalities that affect glial cells (e.g. leukodystrophies) and inflammatory damage to myelin and oligodendrocytes (e.g. multiple sclerosis).<sup>51</sup> Failure in re-myelination predisposes axons to degenerate since a chronic de-myelination leaves denuded neurons vulnerable to atrophy, an irreversible degenerative event that is probably followed by a progressive axonal loss<sup>52</sup> as present in the later stages of *multiple sclerosis* (MS).<sup>53</sup> MS is an inflammatory disease associated with failure in re-myelination. However, in some MS patients there is evidence of complete re-myelination in a significant number of lesions.<sup>54</sup> By now, the reasons for re-myelination failure in MS are not fully understood.

Re-myelination failure can either occur during the recruitment or the differentiation phase. In the recruitment phase the lack in environmental support, a depleted OPC pool or old age<sup>55</sup> could influence activation, proliferation or migration of OPCs<sup>56</sup>, whereas in the differentiation phase the OPCs are somehow restrained to differentiate into a functional, myelinating Oligodendrocyte.<sup>57</sup> According to that, quiescent OPCs have been observed to be present in chronic MS lesions<sup>58,59</sup> presumably caused by differentiation failures after recruitment to the site of lesion.

The re-myelination ability depends on the absence of stimulating or the presence of inhibitory signals in the lesion.<sup>60</sup> Amongst others, such inhibitory signals have shown to be myelin proteins that are present in de-myelination caused debris.<sup>61,62,63,64</sup> In the process of re-myelination, macrophages are important for the removal of this myelin debris since a block of macrophage debris clearance ability results in detained differentiation of OPCs. In aging animals, OPC differentiation is thought to be slowed due to a poor macrophage response that causes a delayed myelin debris clearance.<sup>65,66,67,68</sup>

Based on the inhibitory effect of myelin *in vitro* following experiment was performed to test the impact of the myelin substrates in *in vivo*. Purified central nervous system myelin was supplemented into toxin induced lesions in rats. After day 28, the control group restored myelin but axons of the myelin treated group remained un-myelinated. Notably, the density of OPCs in the lesion was the same in both groups suggesting a normal recruitment of OPCs to the lesion site. Those results indicate the phagocytic clearance of myelin debris after demyelination to be an essential step to ensure effective re-myelination in the CNS and further, that inhibition of OPCs differentiation rather than of OPC recruitment is responsible for re-myelination failure.<sup>63</sup>

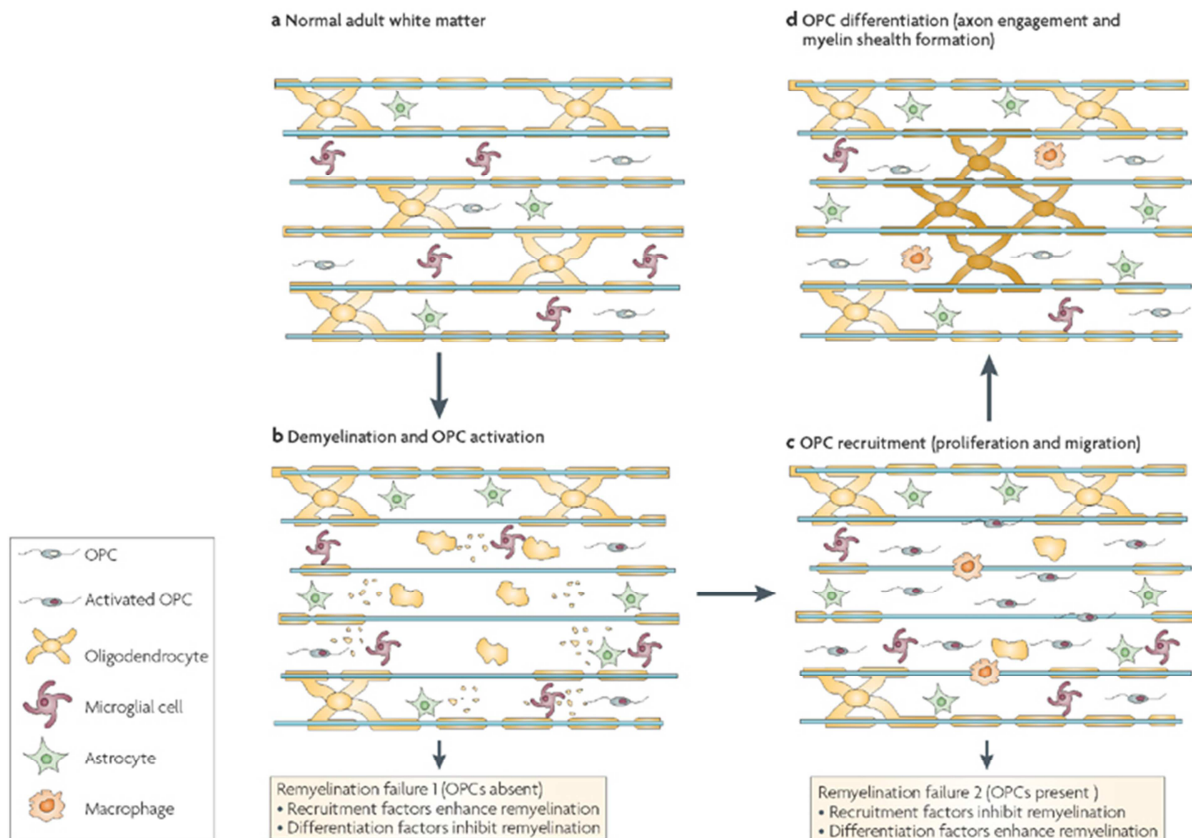


**Figure 4 | a** The normal adult white matter consists of astrocytes, microglia, myelinating oligodendrocytes and OPCs. **b** Subsequently after de-myelination, microglia and astrocytes are activated which in turn activate surrounding OPCs. **c** Macrophages begin to remove the myelin debris. Astrocytes and inflammatory cells secrete mitogens and pro-migratory factors leading the OPCs to proliferate and guide them to the de-myelination site. A failure of OPCs recruitment will end in incomplete or lack of re-myelination. **d** Recruited OPCs will start to differentiate and to produce myelin sheets after axonal contact is established. During this phase, re-myelination generally fails.<sup>39</sup>

Additionally, re-myelination is also influenced by other cell types including astrocytes<sup>69</sup> and lymphocytes.<sup>70</sup> Neighbouring glial cells are thought to activate OPCs from a quiescent into a regenerative state<sup>71</sup>, whereas the differentiation into a myelinating oligodendrocytes depends on the establishing of axonal contact.<sup>9</sup> Those facts disclose a whole network of interacting cells and signals involved in this complex process of myelin repair and suggest that therapeutic strategies will have to be combined for an effective therapy.

## 1.7 Ephrins & Eph-Receptors

Ephrins are membrane bound guidance molecules that function as ligands for their corresponding Eph receptor on neighbouring cells through direct cell to cell contact.<sup>72</sup> Eph receptors have intracellular tyrosine kinases (RTKs) and are divided into EphA and EphB receptors. Upon ligand binding the receptors tyrosine gets auto-phosphorylated followed by activation of the kinase that promotes signal transduction. There are either EphrinA ligands that are bound to the cell membrane by glycosylphosphatidylinositol (GPI) anchors or EphrinB ligands that are transmembrane proteins. With few exceptions, EphA receptors bind EphrinA ligands and EphB receptors bind EphrinB ligands. However, when an EphrinB ligand is bound, bidirectional signals are transduced into both cells since each EphrinB ligand either act as a ligand, sending non cell autonomous signals to adjacent cells or as a receptor, sending cell autonomous signals into the own cell through their intracellular domain and a yet unidentified kinase.<sup>73,74</sup>

The interest in Ephrins and their possible effects on oligodendrocyte differentiation raised because spinal cord injury in rats was followed by up-regulation of Eph-Receptors in astrocytes and neurons<sup>75,76</sup> and EphrinB3 was identified to act like a myelin-based inhibitor of neurite outgrowth.<sup>77</sup>

EphrinB3 is expressed in the region of cortex, hippocampus and amygdala as an integral membrane component of myelin sheaths and recently has been demonstrated to be a potent myelin associated inhibitor of OPC differentiation. When EphrinB3 is fused to an antibodies' Fc-region, EphrinB3 molecules can be clustered by a human IgG antibody and together increase the sensitivity of bound Eph-Receptors to mediate a stronger inhibitory response on OPC differentiation and process formation or OPC lineage progression at later stages.<sup>78, 81</sup>

## Project Overview

Analysing of primary OPCs vs.  
OPC cell lines

EM analysis of myelin  
abnormalities in EphrinB3 knock-  
out mice

EphrinB3 and its receptors

## 2. Project overview

### 2.1 Analysing of primary OPCs versus OPC cell lines

Primary cells are derived directly from tissue of organisms. For the generation of pure primary OPCs, P0-P2 neonatal cortices are digested to form a mixed glia cell culture that has to be incubated for about 10 days. After this period, OPCs can be isolated through a procedure called 'shake off' and have to be seeded immediately afterwards in the according experimental conditions (see figure 5).

When OPCs are incubated in Satos media + 0.5 % FCS, first membranous processes are formed after 4h to 6h and they differentiate into myelinating oligodendrocytes about d3-4. On the other hand, OPC differentiation can be inhibited by *myelin protein extract* (MPE) and by the just recent identified molecule *EphrinB3*.<sup>78</sup> *In vitro* OPC maturation reflects the same stages since *in vivo* suggesting the differentiation capacity to be intrinsic to the OPCs.<sup>7</sup> Therefore, primary OPCs are an adequate model to investigate the OPC differentiation process. However, this procedure of primary OPCs isolation is time-consuming and a considerable amount of P0-P2 rats is necessary to gain a reasonable output. Hence, it is worth to try to reproduce the differentiation experiments of primary OPCs with OPC cell lines in order to reduce animal sacrifices and a faster realization of experiments.

The OPC cell lines OLI-Neu and OLN-93 were selected to investigate their morphology and differentiation potential compared to primary OPCs. After identification of a suitable differentiation media, the inhibitory effect of MPE and EphrinB3 on OLI-Neu and OLN-93 cell differentiation was visualized through double-immunocytochemical staining against the markers O4 & MBP.

## Overview OPC experiments

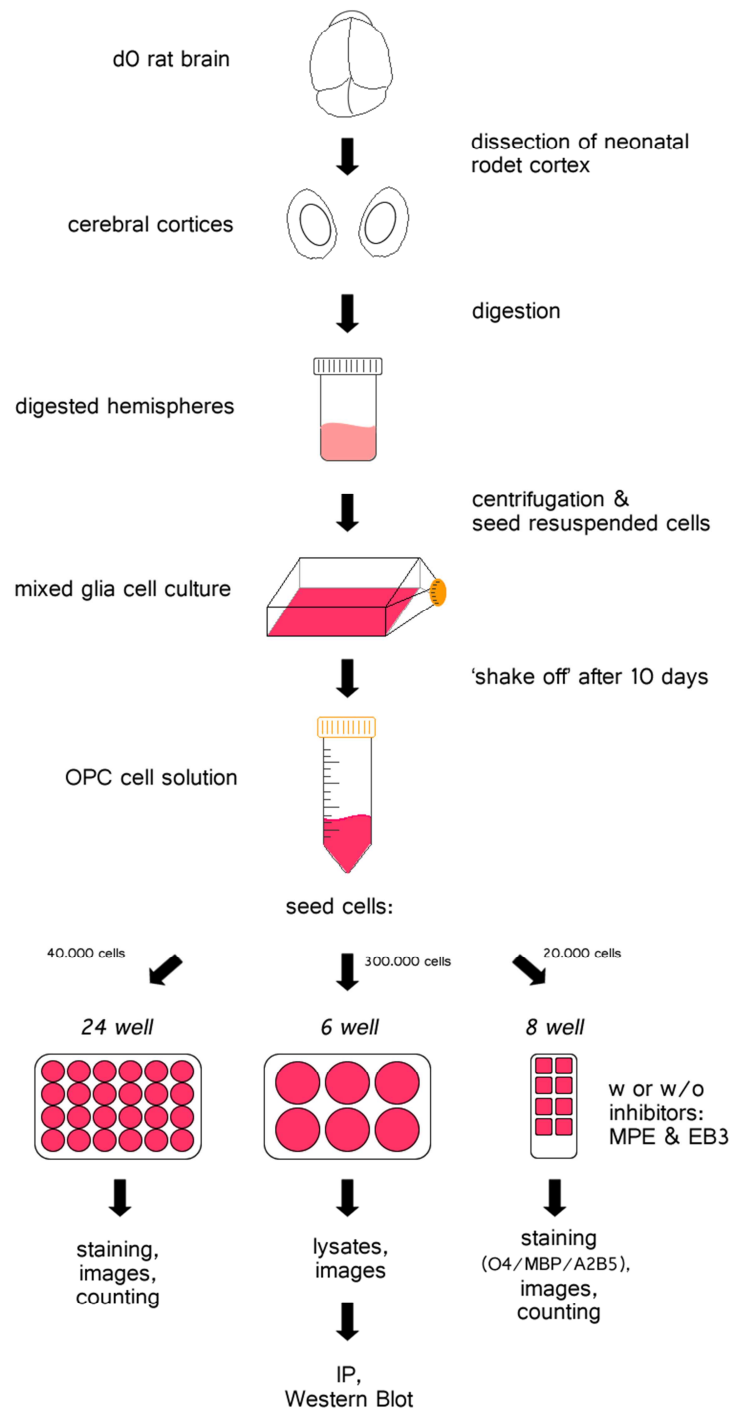


**Figure 5 | Overview of primary OPC experiments.** After purification of primary OPCs from neonatal rat cortices, OPCs were seeded into different media conditions to perform differentiation and inhibitory experiments.



## Overview cell line experiments

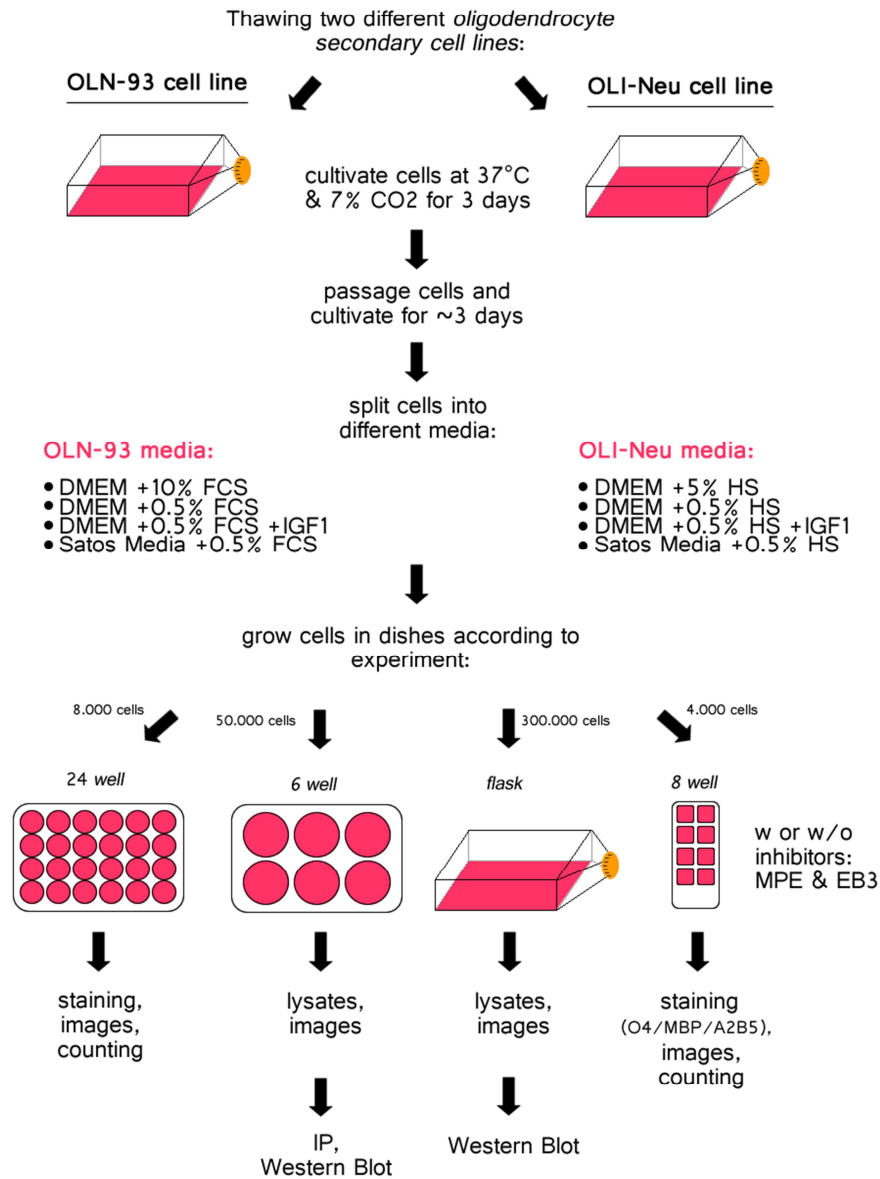
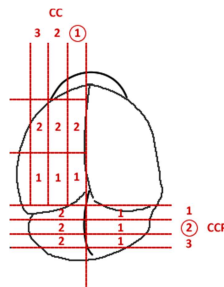


**Figure 6 | Overview of OPC cell lines experiments.** OLI-Neu and OLN-93 cells were seeded into different media conditions to reproduce primary OPC differentiation and inhibitory experiments.

## 2.2 EM analysis of myelin abnormalities in EphrinB3 knock-out mice

As EphrinB3 has shown to inhibit OPC differentiation *in vitro*<sup>78</sup>, the investigation of possible myelin abnormalities in EphrinB3 knockout rats is an obvious interest. Analysis of brain sections by electron microscopy (EM) is an effective method to identify the quality of axon myelination. Therefore, brains of five EphrinB3 knockout rats of different ages (d2, 1M, 3M, 6M, old) and five according control brains were fixed and embedded in resin blocks. For identification of white matter in the caudal cerebellar penduncle (CCP) the blocks were cut with an ultramicrotome (0.2 µm slices) and analysed. The areas of white matter were marked on the block and handed to Mike Peacock (Institute for Neurosciences, Vet. Medicine, Cambridge, UK) who prepared the EM slices for further analysis. Those were photographed and studied for myelin abnormalities through visible phenotypes and determination of the g-ratio. The g-ratio is the ratio of the inner axonal diameter to the total outer diameter and very reliable to assess axonal myelination as it has to be accurate to achieve maximal conduction efficiency and physiological optimization.<sup>50</sup>

### Brain cutting overview:



Encircled numbers represent the preferred specimen for analysing

### Analysed brain specimen:

day 2 (d2) (2 KO & 2 Control brains)	1 month (1M) (1 KO & 1 Control brain)	3 month (3M) (1 KO & 1 Control brains)	6 month (6M) (1 KO & 1 Control brains)	Old (o) (2 KO & 2 Control brains)
<b>Control brain 1:</b> day2 C1 CCP1 day2 C1 CC1  <b>KO brain 1:</b> day2 K1 CCP1 day2 K1 CC1  <b>Control brain 2:</b> day2 C2 CCP1 day2 C2 CC2  <b>KO brain 2:</b> day2 K2 CCP2 day2 K2 CC1	<b>Control brain 5:</b> 1M C5 CCP21 1M C5 CC11  <b>KO brain 5:</b> 1M K5 CCP12 1M K5 CC11	<b>Control brain 7:</b> 3M C7 CCP12 3M C7 CC11  <b>KO brain 7:</b> 3M K7 CCP21 3M K7 CC12	<b>Control brain 6:</b> 6M C6 CCP21 6M C6 CC12  <b>KO brain 6:</b> 6M K6 CCP21 6M K6 CCP11	<b>Control brain 3:</b> o C3 CCP21 o C3 CC11  <b>KO brain 3:</b> o K3 CCP22 o K3 CC11  <b>Control brain 4:</b> o C4 CCP22 o C4 CC12  <b>KO brain 4:</b> o K4 CCP21 o K4 CC12

### 2.3 EphrinB3 and its receptors

As EphrinB3 has shown to be a potential inhibitor of OPC differentiation<sup>78</sup> and IgG clustered EphrinB3 has been identified to activate the Eph receptors B1, B2, B3 and A4<sup>81</sup>, there is an obvious correlation between those facts and a strong interest in finding the Eph receptor(s) mediating this differentiation block. Therefore, the following Eph receptor Phosphorylation Status Assay was performed to investigate the Ephrin mediated pathways of OPC differentiation.

In this experiment, purified OPCs were seeded on 6 well plates and let settled for 4h. After this period, EphrinB3 was added to attached OPCs or not (= control). Lysates were made from both conditions at two time points: 45min and 4h after addition. Out of those lysates, the Eph receptors B1, B2, B3 & A4 were immunoprecipitated. The following detection of tyrosine kinase phosphorylations and according Eph receptor should display the differences within the phosphorylation patterns of the mentioned Eph receptors when EphrinB3 was added or not. Activation of Eph receptors would be visible through additional tyrosine phosphorylation bands.

In addition, EphrinB3 was tried to be immunoprecipitated and detected through western blot method either out of myelin protein extract (MPE) or out of oligodendrocyte lysates as it can function as a receptor as well.

# **METHODS**

**Preparation of OPCs**

**Purification of OPCs**

**Preparation of MPE**

**Protein Determination**

**Immunoprecipitation**

**SDS-Page**

**Western Blot**

**Embedding of brain tissue**

**Immunocytochemistry**

**Others**

### 3. Methods

#### 3.1 Preparation of mixed glial cells (MGCs)

MGCs primary cultures were obtained from P0 to P2 neonatal *Sprague-Dawley Rat* cerebral cortices according to a standard protocol<sup>85</sup> that was adapted from our group.<sup>64</sup> All steps were carried out in a dissection hood with 70% EtOH sterilized instruments. The brains were resected with a curved scissors and collected in a MEM containing petri dish. The following dissection steps were performed: removal of cerebellum, separation of cortices, removal of midbrain (including basal ganglia) and peeling away of meninges. Then, 6/8 cerebral cortices at once were digested with 1 ml sterile filtrated *digestion buffer* for 30 min at 37°C and homogenized before stopping the reaction with the 10 fold volume of preheated DMEM followed by centrifugation at 1500 rpm for 10 min. After discarding of the supernatant the loose pellet was re-suspended in 1 ml DMEM and the cell suspensions plated on PLL coated flasks. These mixed glia cell cultures were cultivated in a 0.01% Poly-L-Lysine (PLL) coated T75 flask with 10 ml DMEM + 1% Penicillin/Streptomycin + L-Glutamine + 10% FCS for about 10 days at 7.5 % CO<sub>2</sub> and 37°C whereas the media was changed every 3 to 4 days.

#### 3.2 Purification of OPCs (Shake-Off)

About 10 days after plating, the mixed glia cell cultures were confluent (astrocyte layer with OPCs and microglia on top). First, the loosely adherent microglia were pre-shaken by agitate flasks for 1h at 37°C and 260 rpm on an orbital shaker. Then, the media was removed and the cells were washed with preheated 1x PBS. Afterwards, 10 ml preheated DMEM was added to cultivation flask followed by a *Shake-Off* of OPCs either per hand or overnight agitation on orbital shaker.

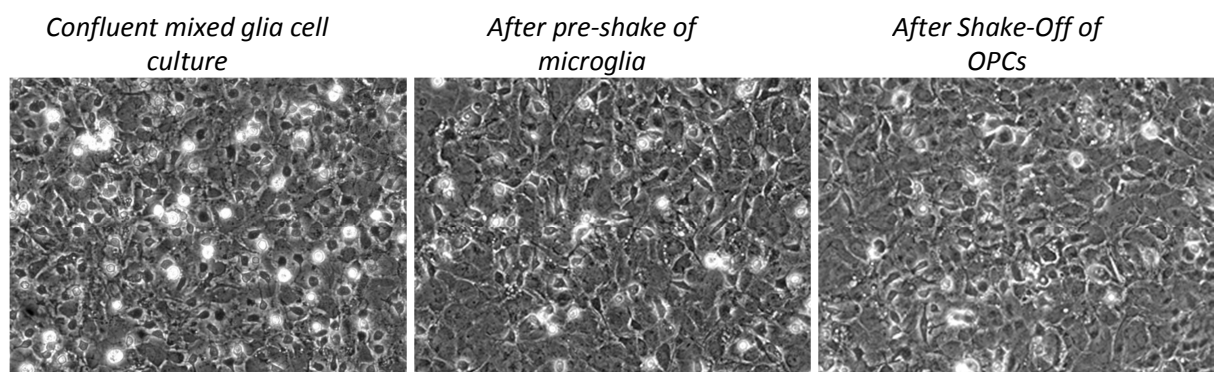


**Figure 7** | image of confluent mixed glia cell culture (**left**), glia cell culture after removal of microglia (**middle**), glia cell culture after shake off of OPCs (**right**). Note: It is possible to shake off OPCs again after cultivation of remained mixed glia culture in 10 ml DMEM for about 1 week. The media should be changed every 3 to 4 days.

The OPC including media was then collected and transferred to an untreated petri dish and incubated for 10 min as contaminating microglia tend to attach more rapidly to petri dish surface than OPCs.

Afterwards the petri dish was swirled gently and the media was pipetted into a 50 ml falcon tube. Finally, the OPC suspension was centrifuged for 10 min at 1000 rpm, the pellet was suspended in 1 ml Satos media and cells were counted using a 'Bright Line Counting Chamber'. For differentiation, OPCs were seeded in Satos Media + 0.5 % FCS on PLL coated dishes at following density: per 8-well (0.9 cm<sup>2</sup>): 25.000 cells and 300 µl media; per 6-well (9.6 cm<sup>2</sup>): 300.000 cells and 3000 µl media, per 24 well: 40.000 cells and 500 µl media. OPCs were incubated at 37°C with 7.5 % CO<sub>2</sub>.

### 3.3 Preparation of myelin membrane substrates and myelin protein extracts

In general, myelin was purified through discontinuous density sucrose gradient centrifugation and osmotic disintegration.<sup>86</sup> All centrifugation steps were carried out with an Ultra-Centrifuge (Avanti J-30I Centrifuge, Beckman Coulter).

Brains of young Sprague-Dawley rats (female) were homogenized mechanically for 2 min in ice-cold 0.32M sucrose using a mechanical blender (Ultra-Turrax; IKA, T18basic). The homogenized brains were diluted with 2.5mM Tris/HCl pH7.0 to a final sucrose concentration of 0.25M and pelleted for 10 min at 55 000 g, 4°C. The pellet was re-suspended in 17 ml of 0.88M sucrose solution and overlaid carefully with 17 ml of 0.25M sucrose solution to establish a gradient. After sucrose density gradient centrifugation for 1h at 100 000 g and 4°C, the myelin interface was collected and mixed in 30 ml of ice cold dH<sub>2</sub>O followed by pelleting for 10 min at 55 000 g and 4°C. The pellet was re-suspended in 10 ml ice cold dH<sub>2</sub>O, the myelin solution incubated for 1 h on ice for osmotic shock and then pelleted again for 10 min at 55 000 g and 4°C. After removal of the supernatant, the flotation and two washing steps were repeated. The pellet was stored at -80°C until isolation of *Myelin Protein Extract* (MPE).

To prepare MPE, the pellets were thawed and re-suspended in 1% N-octyl-beta-D-glucopyranoside, 0.2M Sodiumphosphate pH 6.8, 0.1M Na<sub>2</sub>SO<sub>4</sub> and 1mM EDTA and incubated at 23°C for 2h. Then the solution was centrifuged for 30 min at 100 000 g and 18°C and the supernatants were collected, aliquoted and stored at -20°C until further usage.<sup>63</sup>

For plating of MPE, 40 µg of MPE solution were added onto Poly-L-Lysine-Hydrobromide precoated cell culture dishes over night at 4°C. The next day, the MPE solution was sucked off and OPCs were seeded.

### 3.4 Determination of protein concentration (BCA)

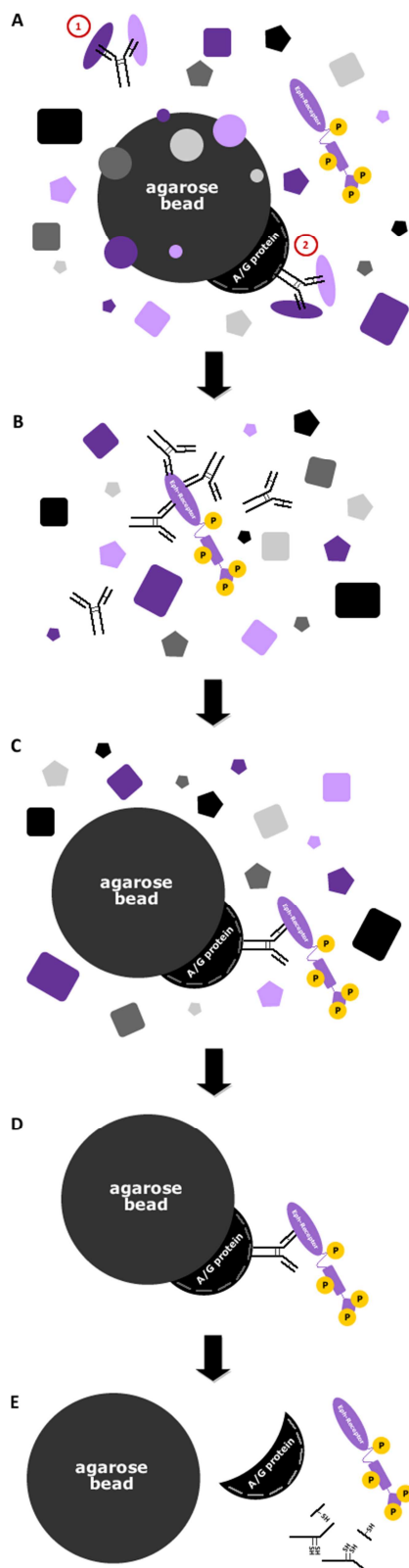
This method includes the *biuret reaction* (reduction of  $\text{Cu}^{2+}$  to  $\text{Cu}^{1+}$ ) with a following highly sensitive and selective colorimetric detection of the cuprous cation ( $\text{Cu}^{1+}$ ) with a reagent that contains *bicinchoninic acid* (BCA). The chelation of two BCA molecules with one cuprous ion forms the purple coloured reaction product which absorbs a wavelength of 562 nm (nearly linear with increasing protein concentration over 20 - 2 000  $\mu\text{g/ml}$ ).

Therefore, the BCA<sup>TM</sup> Protein Assay Kit from *Pierce* was used. Before each measurement, a calibration curve with a BSA standard was performed in advance with following concentrations: 1mg/ml; 0.5 mg/ml; 0.25 mg/ml; 0.125 mg/ml and 0.062 mg/ml. The solutions were prepared according to the data sheet: 50  $\mu\text{l}$  protein solution (blank, or standard) were mixed with 950  $\mu\text{l}$  of *Working Reagent* (50 parts 'Solution A' + 1 part 'Solution B') in a 1.5 ml Eppendorf Cup and put on 37°C with 600 rpm for 30 min. Then, the Eppi was inverted several times and the solution transferred into a semi-micro cuvette. Protein determination was performed with an Eppendorf Bio-photometer at 562 nm. *Note: the protein solution can be diluted with  $\text{dH}_2\text{O}$  or 1x PBS (according to blank).*

### 3.5 Immunoprecipitation

An *immunoprecipitation* (IP) follows the principle of an antigen-antibody reaction. Thereby, a specific antibody against the desired protein is added to a protein-lysate solution. Then, the antibody-protein complexes are precipitated by adding agarose beads with bound A/G-proteins that recognizes the antibodies Fc-Domain. After centrifugation, the protein of interest will be dissolved from the agarose-bead-antibody conjugate through heating in the appropriate SDS-page loading buffer and analysed by immunoblotting.

### 3.5.1 Immunoprecipitation overview



#### A) Preclear

Remove proteins that can cause contamination through unspecific binding to agarose beads or AB:

① 1  $\mu$ g of Ms IgG antibody was added to lysate and rotated for 15 to 30 min at 4°C. ② Then, 10 to 20  $\mu$ l protein A/D agarose beads PLUS (Millipore) were added to the cell lysate and rotated 30 min at 4°C ( $\rightarrow$  the immobilized A/G protein on the agarose beads surface will bind the IgG antibodies Fc-region). After centrifuging for 5 min at 2500 rpm and 4°C the supernatant was transferred into a new eppendorf cup.

#### B) Target protein of interest with according antibody:

1  $\mu$ g of according antibody were added to lysates. As a negative control, the same amount of IgG antibody was used for 'control lysate'. The antibody-protein solutions were rotated for about 1-2h at 4°C.

#### C) Pull down protein of interest:

10 to 20  $\mu$ l of protein A/G agarose beads PLUS were added to antibody-protein solutions and rotated over night at 4°C.

#### D) Wash beads to remove unbound proteins:

Centrifugation for 5 min at 2500 rpm and supernatant was removed. Following washing step with 500  $\mu$ l of ice cold 1xPBS or IP washing buffer (+ Protease Inhibitor + Phosphatase Inhibitor) was repeated 4x.

#### E) Dissolve protein-bead complexes:

The protein-bead complexes were dissolved by adding 20 to 40  $\mu$ l of 1x SDS-Page loading buffer and heating for 3-5 min at 99°C and 750 rpm (Di-sulfide-bonds will be reduced and protein-aggregates dissolved).

Afterwards, agarose beads were spinned down and 10 to 20  $\mu$ l of protein-buffer solution were loaded on a Tris-Gly-Gel for following SDS-Page.

**Figure 8| Illustration of an IP for Eph receptors.** Note that IP was also performed on EphrinB3 proteins.



### 3.6 SDS-Page

For separation of proteins in a mass weight (Mw) dependent way, it is necessary to denature them and mask their natural charge. The detergent **SDS** (sodium dodecyl sulphate) was used to destroy the proteins hydrogen bonds and to cover the proteins natural charge with a negative one → the bigger the protein, the more negative charge is present. Beta-Mercaptoethanol was used to reduce the proteins di-sulfide bounds (heating for 3-5 min at 99°C enhances the process).

The proteins were then separated by using **polyacrylamide gel electrophoresis** (tris-glycine gels and electrophoresis-chamber from Invitrogen) in an appropriate electrolyte containing buffer (*SDS-running-buffer*). After applying of voltage (135 V, 35 mA), all proteins will be attracted by the positive pole as they are negatively charged. Lighter proteins will migrate much faster through the gel than heavier ones as the acrylamide grid functions as a barrier. Therefore, the speed of migration can be regulated through a variable percentage of acrylamide.

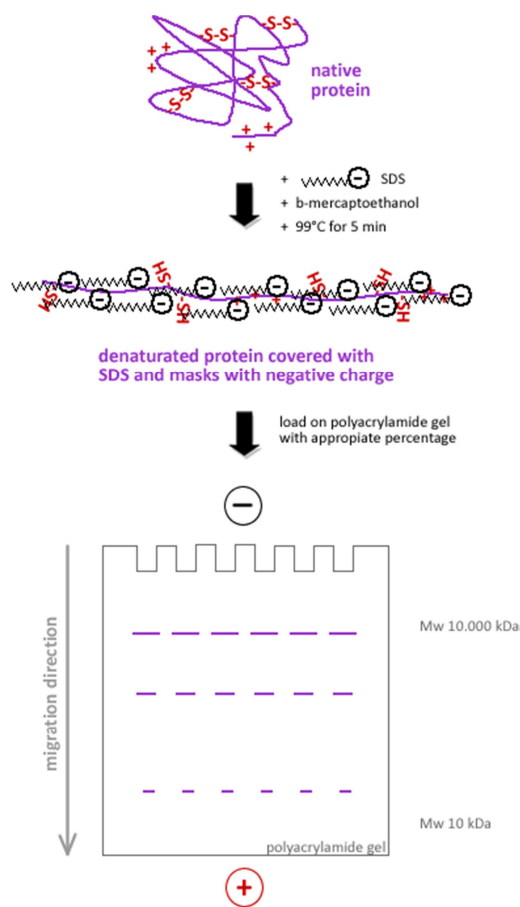
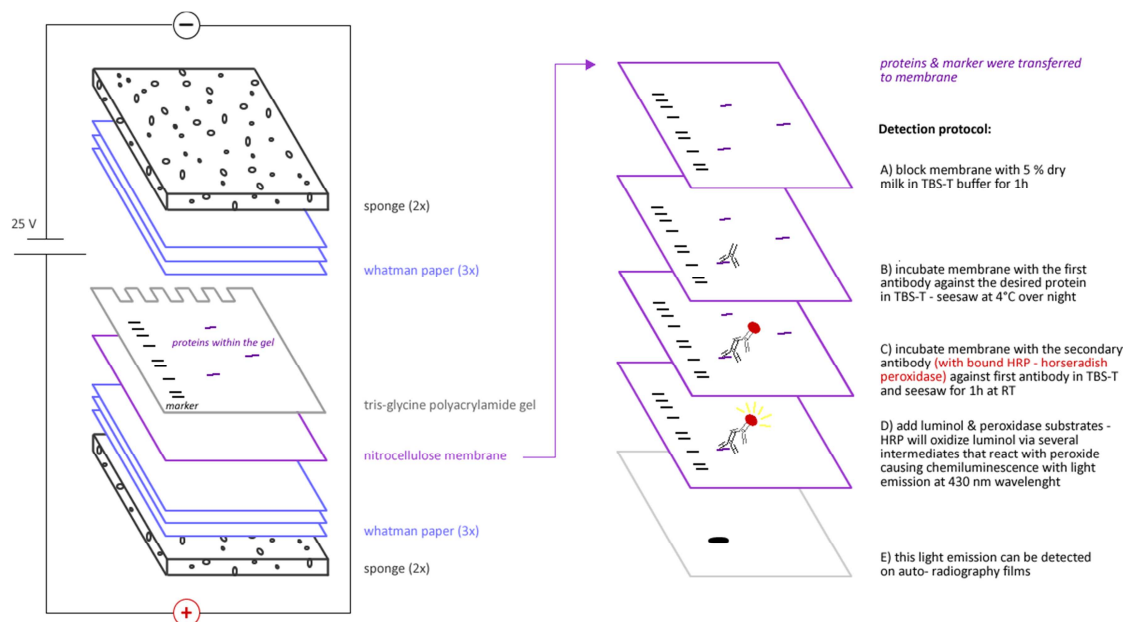


Figure 9 | SDS-Page overview.

### 3.7 Western-Blot

After SDS-Page, the separated proteins within the gel were transferred to a nitrocellulose membrane (Hybond ECL from Amersham) in a blocking chamber from invitrogen. Therefore, the proteins were forced to migrate out of the gel onto the membrane by applying of vertical voltage in an appropriate *Transfer Buffer*. As the proteins are negatively charged, it is important to put the membrane between gel and positive pole – see *figure* for assembly of blotting apparatus and procedure.

For enhanced chemi-luminescence (ECL), the *Amersham ECL Plus Western Blotting Detection System* was used. Oxidation of Lumigen® PS-3 through HRP generates numerous acridinium ester intermediates per minute which react with peroxide at alkaline pH and produce high-intensity chemiluminescence. This light emission at 430 nm was detected on autoradiography films (*Amersham Hyperfilm™ ECL*).



**Figure 10 | Western Blot overview.** Assembly of blotting apparatus and procedure for chemi-lumineszenz.

### 3.8 Embedding of brain tissue

Wild type and Knock out rat brains were cut (Figure 11 | A) and the tissue placed into basket chambers in appropriate order (Figure 11 | B). Six baskets at once were strung and fixed on a stab (Figure 11 | C), transferred into a bijou tube and rotated in 2% osmium over night at 4°C (Figure 11 | D).

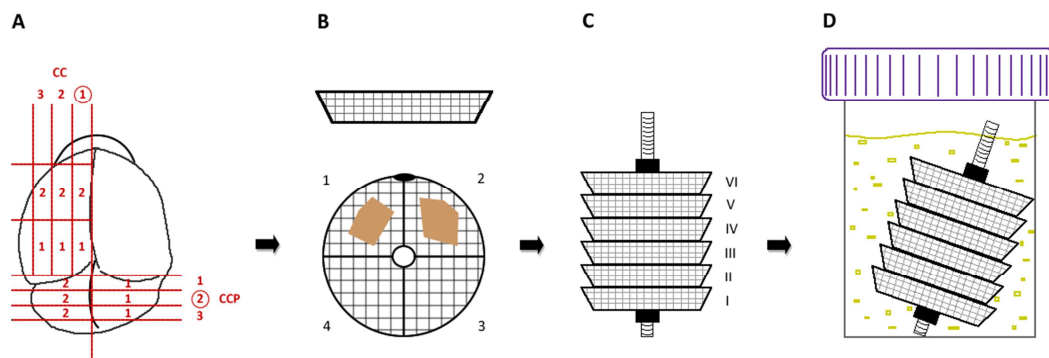


**Figure 11 | Overview of brain tissue embedding.** A Brain cutting procedure, B-C Embedding procedure.

The next morning, the osmium solution became black and baskets were washed twice with dH<sub>2</sub>O. Then, baskets were washed with 70% EtOH for 15 min, 95% EtOH for another 15 min and 100% EtOH for 3x 10 min. Afterwards, propylene oxide was added for 2x 15 min, discarded and specimen left in a 50:50 propylene oxide & resin mix overnight, rotating. Baskets were then rotated in a 100% resin mix for at least 6hs followed by embedding of the specimen in a new 100% resin mix. Therefore, the tubes had to be filled with two drops of 100% resin mix, then, the specimen was placed in desired cutting

direction and the tube filled up with 100% resin mix. This procedure was repeated for all specimen and tubes were stored in the oven at 60°C for polymerization overnight. The hard resin blocks were freed by cutting off the plastic tube:



**Figure 12 | Preparation of resin blocks.**

### 3.9 Preparing of EM-slices

An ultramicrotome was used to cut the resin blocks. The blocks were first trimmed with a rasp until tissue was reached. With a glass knife, the tissue was trimmed to obtain a plane surface and a fresh glass knife was used to cut 1-2  $\mu\text{m}$  slices – when water is dropped on the glass knife, the surface tension will avoid screwing of slice – and placed upon a water drop spotted on a microscope slide. Some slices were collected on one slide and put on a heater dish for vaporization of the water drop causing the slice to stick. Thereafter, the slices were stained with methylene blue by heating the slide for two seconds above a Bunsen burner, adding methylene blue and heating the slide again for 3 seconds above the Bunsen burner. Thereby, the methylene blue solution must not cook. Then, the slide was washed with hot water upside-down and dried on a heater dish overnight.

The stained slices were analysed under a light microscope where grey matter regions can be identified and marked on the resin block for electron microscope section preparation (performed by Mike Peacock, Neurosciences, Vet.Medicine, Cambridge, UK). The electron microscope sections were then analysed and photographed with a HITACHI H600 transmission electron microscope at different magnifications.

### 3.10 Immunocytochemistry

The *immunocytochemistry staining* follows the principle of an antigen-antibody reaction. Thereby, a specific antibody against the desired protein is added to previously fixed cells. This first antibody can be detected through a secondary antibody with a bound fluorochrome at the right wavelength.

#### 3.10.1 Fixation of cells

The media was removed and cells washed twice with pre-incubated 1x PBS. Fixation of cells occurred through addition of 4% PFA for 10 min followed by washing two times with 1x PBS.

#### 3.10.2 Blocking/permeabilisation step

*Solution A* was added for 5 min.

### 3.10.3 Staining

The cells were stained with the first antibody against the desired protein and appropriately diluted in *Solution B* for one hour at RT or overnight at 4°C (*note: the antibody dilution was decreased when incubated overnight*). Then, cells were washed three times with 1x PBS for 5 min before incubation with the according secondary antibody diluted in *Solution B* for one hour at RT. The cells were washed again with 1x PBS three times for 5 min (*note: double staining is possible by repeating this protocol with another 1<sup>st</sup> antibody*). Afterwards, the nuclei were stained with dapi diluted in *Solution B* for 2 min at RT and washed again with 1x PBS. Pictures were taken with an Olympus BX 71 microscope.

<b>1<sup>st</sup> antibodies</b>	<b>dilutions</b>	<b>2<sup>nd</sup> antibodies</b>	<b>dilutions</b>
<b>Anti-O4</b> Millipore	ICC: 4,5 µl/ml (10-20 µg/nl)	<b>Anti-Ms Cy3</b> Jackson Immuno Research	10 µl/ml
<b>Anti-MPB</b> Chemicon	ICC: 6µl/ml	<b>Anti-Rt Cy2</b> Jackson Immuno Research	10 µl/ml
<b>Anti-EphB1</b> R&D	WB: 10 µl/10ml	<b>Anti-Rt</b>	1:2500
<b>Anti-EphB2</b> R&D	WB: 0,2 µg/ml ICC: 10 µg/ml	<b>Anti-Ms</b> <b>Anti-Ms Cy3</b> Jackson Immuno Research	1:2500 10 µl/ml
<b>Anti-EphB3</b> Abcam	WB: 7 µl/15ml (1:500 – 1:1000)	<b>Anti-Rb</b>	1:2500
<b>Anti-Eph4A</b> Abgent	WB: 10 µl/10ml 1:100-500	<b>Anti-Rb</b>	1:2500
<b>Anti-Phosphotyrosine</b> Millipore	WB: ~ 0,1 µg/ml	<b>Anti-Ms</b>	1:2500
<b>Anti-A<sub>2</sub>B<sub>5</sub></b> Chemicon	ICC: 5µl/ml (5-10µg/ml)	<b>Anti-Ms Cy3</b> Jackson Immuno Research	10 µl/ml
<b>Anti-nkx2.2</b> Aviva	WB: 1,25 µl/10ml	<b>Anti-Rb</b>	1:2500
<b>Anti-GAPDH</b> Abcam	WB: 0,5-1 µg/ml	<b>Anti-Rb</b>	1:2500
<b>Anti-alpha-Tubulin</b> Abcam	WB: 1:5000-10000	<b>Anti-Ms</b>	1:2500
<b>Anti-GaIC</b> Millipore	ICC: 1:10-50	<b>Anti-Rb Cy2</b> Jackson Immuno Research	10 µl/ml
<b>Anti-PLP</b> Abcam	ICC: 1/100	<b>Anti-Ms Cy3</b> Jackson Immuno Research	10 µl/ml

### 3.11 Differentiation of OLN-93 and OLI-Neu cell lines

After proliferation about 2-3 days, the cell lines were passaged and seeded on poly-L-lysine coated dishes and cultured in diverse conditions to define an appropriate differentiation media. Afterwards, they were tested for reproducibility of established primary oligodendrocyte experiments (c.p. figure 6).

**Media overview for OLN-93:**

Satos media + 0.5% FCS

DMEM + 0.5% FCS + IGF1

DMEM + 0.5% FCS

DMEM + 10% FCS (=cultivation media as a control)

**Media overview for OLI-Neu:**

Satos media + 0.5% HS

DMEM + 0.5% HS + IGF1

DMEM + 0.5% HS

DMEM + 5% HS (=cultivation media as a control)

One media contained the Insulin like growth factor 1 (IGF-1) as binding to the IGF-1 receptor is known to play a vital role in Oligodendrocyte development, survival and myelin genesis<sup>79,80</sup> and therefore, probably promotes differentiation. However, the Satos media already included 10µg/ml Insulin.

**Plating overview OLN-93**per 8-well (0.9 cm<sup>2</sup>): 5.000 cells, 300 µl mediaper 6-well (9.6 cm<sup>2</sup>): 10.000 cells, 3 ml media

per T57 flask: 250.000 cells, 10 ml media

**Plating overview OLI-Neu**per 8-well (0.9 cm<sup>2</sup>): 7.000 cells, 300 µl mediaper 6-well (9.6 cm<sup>2</sup>): 20.000 cells, 3 ml media

per T57 flask: 350.000 cells, 10 ml media

The media were changed every 2-3 days. Day1 to Day4 differentiated OLN-93 and OLI-Neu cells were counted, photographed (Olympus BX 71), stained by immunofluorescence for maturation markers, lysed for protein expression analysis and compared to identify the best differentiation media.

**3.12 Others****3.12.1 Harvesting of OLN-93 & OLI-Neu cell lines from flasks**

The cells were washed with warm 1x PBS and incubated with 2 ml 0.05 % Trypsin in DMEM for 2-5 min at 37°C. The reaction was stopped by adding 10 ml pre-warmed DMEM followed by centrifugation at 1500 rpm for 10 min. The supernatant was removed, the cells were diluted in 1 ml pre-warmed Satos or DMEM media with the appropriate percentage of FCS or HS and counted.

**3.12.2 Thawing of OLN-93 & OLI-Neu cell lines**

Cells were immediately transferred from the -80°C fridge (or -140°C liquid nitrogen) in a 37°C warm water bath. As soon as the cell solution was thawed, 10 ml of warm media (DMEM + 10% FCS + L-Glu + P/S) was added drop wise and inverted gently. After spinning at 1000 g for 5 min, the supernatant was decanted and the pellet dissolved in 1 ml warm media. Then, cells were transferred into the flask and incubated at 37°C and 7.5% CO<sub>2</sub>.

### 3.12.3 Freezing of OLN-93 & OLI-Neu cell lines

For freezing cells, they were known to grow well or to be in the log phase. After harvesting and counting of cells, they were centrifugated for 5 min at 1500 rpm. Then, the supernatant was removed and per  $1 \times 10^6$  cells 1 ml of *freezing solution* was added. The cells were re-suspended thoroughly, transferred into cryovials (1 ml) and maintained on ice for approximately 30 min. Keep cells in the  $-80^{\circ}\text{C}$  freezer for short term storage or at least 24 hours before transfer in liquid nitrogen for long term storage.

### 3.12.4 Cell number calculation

Therefore, a 'Bright Line Counting Chamber' was used. Cells were pelleted at 15000 rpm for 10 min and after removal of supernatant (well) dissolved in 1 ml pre-incubated DMEM. 10  $\mu\text{l}$  of cell solution was diluted with 10  $\mu\text{l}$  of Trypan Blue (stains only dead cells) and add 10  $\mu\text{l}$  of Trypan Blue cell solution onto the counting chamber. The cells of three squares were counted and dead cells were subtracted from total cell number. The average of all three squares multiplied by the dilution factor (1:2)  $\times 10^4$  reflects the cell number of living cells in 1 ml.

### 3.12.5 Clustering of EphrinB3

EphrinB3 was dissolved in 1x PBS to a concentration of 200  $\mu\text{g}/\text{ml}$ . The anti-human Fc-IgG (1mg/ml) was mixed with the EphrinB3 solution (4 $\mu\text{l}$  IgG per 200 $\mu\text{l}$  EphrinB3 solution) and allowed to incubate for 3 hours on ice.

# Materials

Primary OPCs

Cell lines

Media

Buffers

Solutions

Chemicals

## **4. Materials**

### **4.1 Primary OPCs**

Mixed glia cell cultures were obtained from P0 to P1 neonatal *Sprague-Dawley Rat* cerebral cortices according to a standard protocol<sup>87</sup> that was adapted from our group.<sup>64</sup> OPCs were purified the *Shake-Off* method and seeded on PLL coated dishes with the according condition.

### **4.2 OPC cell lines**

#### **4.2.1 OLI-Neu**

The OPC cell line, OLI-Neu (provided by J. Trotter, University of Mainz, Mainz, Germany) was first described in 1989.<sup>87</sup> OLI-Neu are cell lines of murine oligodendroglial precursor cells immortalized by an activated tyrosine kinase.<sup>88</sup> For all experiments passage numbers < 30 were used. After passaging, the cells were seeded on PLL coated dishes in Satos media supplemented with 5% HS for cultivation or 0.5% HS for differentiation and maintained at 37°C and 7.5% CO<sub>2</sub>. OLI-Neu cells were passaged 1:5 two or three times a week.

#### **4.2.2 OLN-93**

OLN-93 rat oligodendroglia cells (provided by C. Richter-Landsberg, University of Oldenburg, Oldenburg, Germany) were cultured as described previously from C. Richter-Landsberg & M. Heinrich. They established this permanent cell line, derived from spontaneously transformed cells in primary rat glial cultures.<sup>89</sup> After passaging (only passages <30 were used) the cells were seeded on PLL coated dishes in DMEM supplemented with 10% FCS for cultivation or in Satos media with 0.5% FCS for differentiation and maintained at 37°C and 7.5% CO<sub>2</sub>. OLN-93 cells were passaged 1:8-1:10 two or three times a week for cultivation.

### **4.3 EphrinB3 knock-out mice**

The EphrinB3 knock-out mice have been provided by Prof. Amparo Acker-Palmer.



## 4.4 Cell Culture Media

### 4.4.1 OLI-Neu Cultivation Media

500.00 ml DMEM + 4.5 g/l D-Glucose + 3.7 g/l NaOCO<sub>2</sub>  
5.00 ml Satos Stock Solution (1%)  
25.00 ml heat inactivated Horse Serum (5%)  
5.00 ml Pen/Strep solution (1% / 5000U/ml)  
11.00 µl 10 mM Na Selenite Stock (f.c. 220 nM)  
500.00 µl 100 mM Putrescine Stock (f.c. 100 µM)  
10.00 µl 10 mM Progesterone Stock (f.c. 200 nM)  
2.50 µl 1 mM Tri-Iodo-thyroxine (T3) Stock (f.c. 50 pM)  
26.00 µl 1 mM L-Thyroxine (T4) Stock (f.c. 520 nM)  
1.00 ml 5 mg/ml Insulin solution – fresh (f.c. 10 µg/ml)  
1.00 ml 2,5mg/ml Holo-Transferrin solution – fresh (f.c. 5 µg/ml)  
500.00 µl 100 mM Pyruvate Stock (f.c. 0.11 mM)  
10.00 ml 200 mM L-Glutamine (f.c. 4 mM)

### 4.4.2 OLI-Neu Differentiation Media

500.00 ml DMEM + Glucose + NaOCO<sub>2</sub> or Satos Media  
50.00 ml heat inactivated HS (0.5% or 1%)  
5.00 ml Pen/Strep (1%)  
10.00 ml 200 mM L-Glutamine (f.c. 4 mM)

### 4.4.3 OLN-93 Cultivation Media

500.00 ml DMEM + Glucose + NaOCO<sub>2</sub>  
50.00 ml heat inactivated FCS (10%)  
5.00 ml Pen/Strep (1%)  
10.00 ml 200 mM L-Glutamine (f.c. 4 mM)

### 4.4.4 OLN-93 Differentiation Media

500.00 ml DMEM + Glucose + NaOCO<sub>2</sub> or Satos Media  
50.00 ml FCS (0.5%)  
5.00 ml Pen/Strep (1%)  
10.00 ml 200 mM L-Glutamine (f.c. 4 mM)

### 4.4.5 MEM

500.00 ml MEM  
5.00 ml Pen/Strep solution (1%)  
10.00 ml 200 mM L-Glutamine (f.c. 4 mM)

### 4.4.6 Satos Media

500.00 ml DMEM  
5.00 ml Satos Stock Solution (1%)  
5.00 ml Pen/Strep solution (1%)  
1.00 ml 25mg/ml Holo-Transferrin fresh (f.c. 10 µg/ml)  
1.00 ml 2.5 mg/ml Insulin solution– fresh (f.c. 10 µg/ml)  
10.00 ml 200 mM L-Glutamine (f.c. 4 mM)

### 4.4.7 OPC differentiation Media

Add 2.50 ml FCS (0.5%) into Satos Media

## 4.5 Buffers

### Buffer

**TBS (Tris Buffered Saline) 10x**

**TBS-T 1x**

**SDS-Gel Running Buffer 10x**

**SDS-Gel Running Buffer 10x**

**Transfer Buffer 10x, 1L**

**Transfer Buffer 1x for blotting,  
500ml**

**Blocking Buffer, 10ml**

**Lysis Buffer for IP**

**Wash Buffer for IP**

**MPE Buffer, 10 ml**

### Recipe

20 mM Tris-base

0.9% NaCl

Adjust pH to 7.4 with HCl

Dilute TBS 10x 1:10 with dH<sub>2</sub>O and add 0,1% Tween20

30.3 g Tris base

144.0 g Glycine

10.0 g SDS

Fill up to 1L with dH<sub>2</sub>O

Dilute SDS-Gel-Running Buffer 10x 1:10 with dH<sub>2</sub>O

2.4 g Tris base

14.2 g Glycine

1 ml SDS (10%)

Fill up to 1L with dH<sub>2</sub>O

50 ml Transfer Buffer 10x

350 ml dH<sub>2</sub>O

100 ml Methanol

5 g dry milk (5%)

100 ml TBS-T

Mix for at least 30 min

#### IP Buffer I (Sasha):

0.05 g Octyl Pyranoside (1%)

1.5 ml NaCl (150 mM)

10 µl EDTA (1mM)

Adjust to 5 ml with Tris base (50 mM) pH 8

#### IP Buffer II (Millipore):

0.05 g Octyl Pyranoside (1%)

25 mM Hepes pH 7.5

150 mM NaCl

1 mM EDTA

2% Glycerol

Dilute 1:5 by adding 4ml dH<sub>2</sub>O to 1ml Buffer II

#### IP Buffer III (Yasir):

0.05 g Octyl Pyranoside (1%)

0.2 M Sodiumphosphate pH 6.8

0.1 mM Na<sub>2</sub>SO<sub>4</sub>

1 mM EDTA

#### 25 ml:

1.25 ml Tris (50mM), pH7,6

7.5 ml NaCl (150mM)

100 µl EDTA (2mM), pH 8

50 µl NP-40 (0.2%) or Tween20

10 µl Proteinase Inhibitor

10 µl Phosphatase Inhibitor

0.1 g Octylglycoside

4 ml 0.5 M Sodiumphosphate pH 6.8

1 ml 1 M Na<sub>2</sub>SO<sub>4</sub>

20 µl 0.5 M EDTA pH8

60 µl 0.1 M DTT

5 ml dH<sub>2</sub>O

## 4.6 Solutions

Used formulars:

$$n \text{ (mol)} = m \text{ (g)} * M \text{ (g/mol)}$$

$$V_1 \text{ (ml)} * c_1 \text{ (mg/ml)} = V_2 \text{ (ml)} * c_2 \text{ (mg/ml)}$$

[illegible]

Solution	Recipe
<b><i>Digestion Solution, 10 ml</i></b>	450.00 µl <i>Papain</i> (dissolves the ECM) 150.00 µl <i>DNAse I typeIV</i> 100.00 µl <i>L-Cysteine</i> 9.3 ml <i>MEME</i> (minimum essential medium eagle) → vortex → sterilisation per filter (0.2 µm)
<b><i>Sato's Stock solution</i></b>	5.1 g BSA V 3.0 mg Progesterone 805 mg Putrescine 0.25 mg Sodium Selenite 20 mg T3 (dissolve in 0.1M NaOH in 75%MeOH) 20 mg T4 (dissolve in 0.1M NaOH in 75%MeOH) Adjust to 500 ml in DMEM, make 5 ml aliquots, store at -80°C
<b><i>SolutionA, 15 ml (for Immunocytochemistry)</i></b>	500.00 µl normal goat serum (f.c. 10%) 50.00 µl Triton-X 100 30% (f.c. 0.3%) 4.35 ml 1x PBS → rotate 1h at 4°C to dissolve Triton-X 100
<b><i>SolutionB, 5 ml (for Immunocytochemistry)</i></b>	100.00 µl normal goat serum (f.c. 2%) 16.67 µl Triton-X 100 30% (f.c. 0.1%) 4.85 ml 1x PBS → rotate 1h at 4°C to dissolve Triton-X 100
<b><i>4% Paraformaldehyde Solution (PFA)</i></b>	Dilute 16% PFA-stock 1:4 with PBS 1x
<b><i>Stripping Solution</i></b>	62.5 mM Tris-HCL pH 6.8 100 mM beta-Mercaptoethanol 2% SDS
<b><i>Freezing Solution</i></b>	90% FCS or HS 10% DMSO Add $1 \cdot 10^6$ OLN-93 cells / 1ml Freezing Solution (FCS) Add $2 \cdot 10^6$ OLN-93 cells / 1ml Freezing Solution (HS)

## 4.7 Chemicals

Acetic Acid	Sigma-Aldrich
BSA (Bovine Serum Albumin Fraction V)	Sigma-Aldrich
Bromphenol blue	Sigma-Aldrich
DNAseI Type IV	Sigma-Aldrich
DMEM (Dulbecco's Modified Eagle Medium)	Sigma-Aldrich
DTT (Dithiothreitol)	Sigma-Aldrich
ECL Western Blotting Detection Kit	Amersham
EDTA	Sigma-Aldrich
Ethanol	MERCK
FBS (Fetal Bovine Serum)	Sigma-Aldrich
HCl 37%	Sigma-Aldrich
Hoechst solution	Sigma-Aldrich
HS (Horse Serum)	Sigma-Aldrich
(recombinated) Human EphrinB3	R&D Systems
Human Holo-Transferrin	Sigma-Aldrich
Insuline	Sigma-Aldrich
IGF1 (Insulin Like Growth Factor)	Sigma-Aldrich
L-Cysteine Hydrochloride	Sigma-Aldrich
L-Glutamine	Sigma-Aldrich
Glycerine	Sigma-Aldrich
MEM (Modified Eagle Medium)	Sigma-Aldrich
Mercaptoethanol	Sigma-Aldrich
Methanol	MERCK
Normal Goat serum	Sigma-Aldrich
NP-40	Sigma-Aldrich
Octyl-beta-D-Glycopyranoside	FLUKA
Page Ruler™ Prestained Protein Ladder Plus	Fermentas
10x PBS (Phosphate Buffered Sialine)	Invitrogen
Papain	Worthington
Penstrep (Penicillin-Streptomycin)	GIBCO
PFA (Paraformaldehyde)	Sigma-Aldrich

PMSF (Phenylmethylsulfonylfluorid)	Sigma-Aldrich
Protease Inhibitor Mix	Roche
Poly-L-Lysine-Hydrobromide	Sigma-Aldrich
Progesterone	Sigma-Aldrich
Putrescine (1,4-Diaminobutane)	Sigma-Aldrich
SDS	Sigma-Aldrich
SDS-Page 12,5%	Invitrogen
Sodium Chloride	Sigma-Aldrich
Sodium Hydroxide	Sigma-Aldrich
Sodium Selenite Anhydrous	Sigma-Aldrich
Sucrose	Sigma-Aldrich
T3 (3,3',5-Triiodo-L-Thyronine Sodium Salt)	Sigma-Aldrich
T4 (L-Thyroxine)	Sigma-Aldrich
Tris base	Sigma-Aldrich
Triton X-100	Sigma-Aldrich
Trypan Blue Solution	Sigma-Aldrich
Tween 20	Sigma-Aldrich

## Results

Primary OPCs vs. OPC cell lines

Potential OPC astrocyte switch

EM analysis of EphrinB3 KO mice

Analysis of EphrinB3 and its receptors

## 5. Results

### 5.1 Primary OPCs vs. OPC cell lines

#### 5.1.1 Analysis of primary OPC morphology and differentiation potential.

When primary OPCs were seeded on PLL coated dishes with Satos media + 0.5% FCS, the cells started to form processes after 4h. Those mono- or bipolar progenitors continued in process formation and about 24h, multipolar and slightly branched phenotypes referred to pre-oligodendrocytes were observed. Growth and extensive branching indicated the maturation of oligodendrocytes and first myelin sheets were identified through bright field analysis at d3. The appearance of myelin demonstrated a successful differentiation of OPCs into mature, myelinating oligodendrocytes.

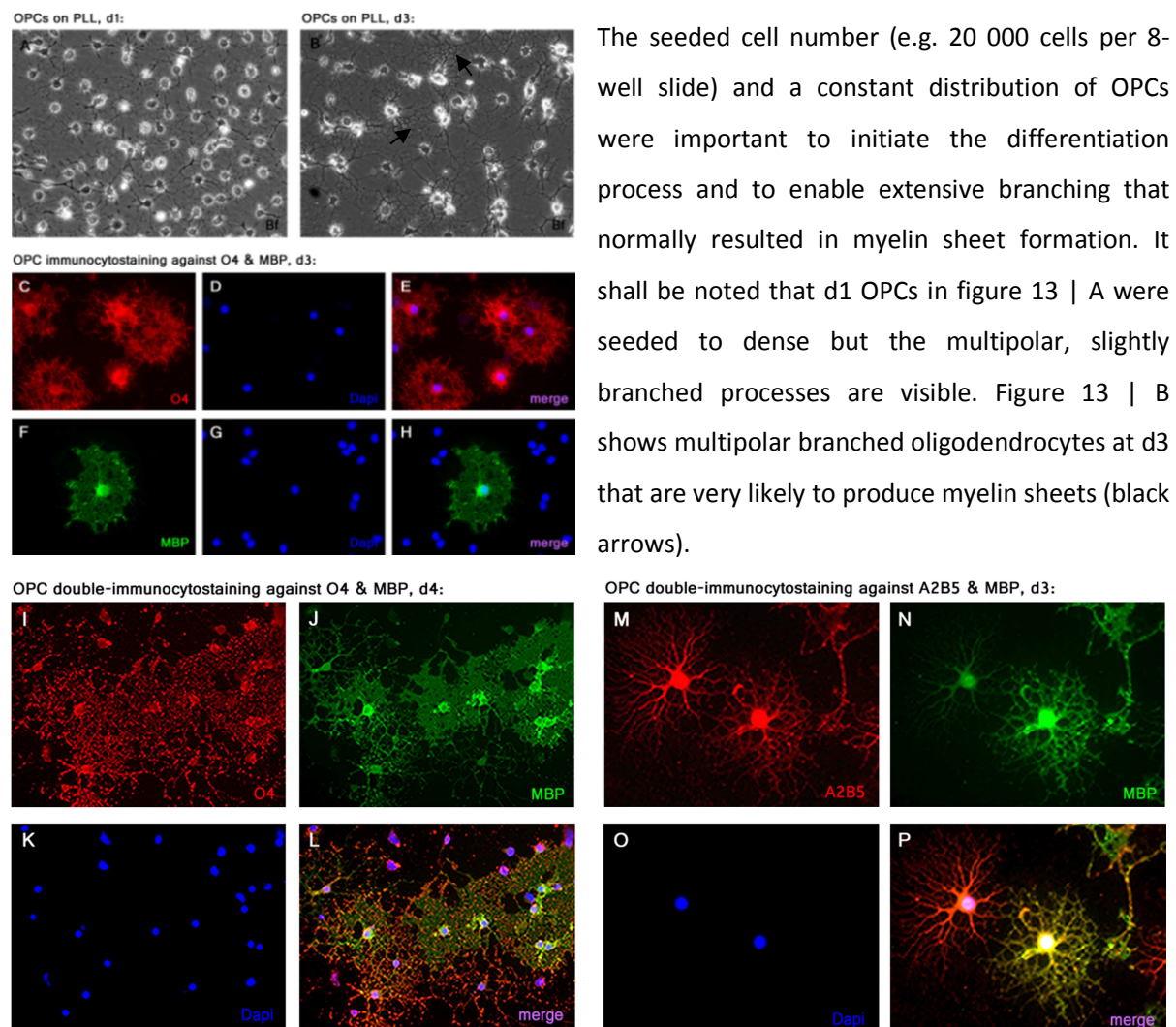


**Figure 13 | Overview of primary OPC differentiation experiments.** **A** bright field image of OPCs with multipolar processes and slightly branching at d1. **B** several multipolar branched, myelin producing oligodendrocytes at d3. **C-E** oligodendrocytes positive for O4. **F-H** oligodendrocyte with wide myelin-sheet formation, positive for MBP. **I-L** oligodendrocytes double-immunocytochemistry against O4 and MBP. The correct distribution of OPCs encourages extensive branching and wide myelin sheet formation. **M-P** oligodendrocytes double-immunocytochemistry against A<sub>2</sub>B<sub>5</sub> and MBP. Stainings against A<sub>2</sub>B<sub>5</sub> enable a definite morphology analysis of branched processes. Note that the right cell is already MBP<sup>+</sup>.



To illustrate the differentiation potential of primary OPCs and their whole extent of branching, the oligodendrocytes were immunocyto stained against the common pre-oligodendrocyte marker *O4* (figure 13 | C,E,I & L). To visualize myelin sheets and to determine fully differentiated primary oligodendrocytes, the myelin marker MBP was used (figure 13 | F-P). Stainings against the general glial cell marker *A<sub>2</sub>B<sub>5</sub>* enabled a definite illustration of branched processes and were used for morphology analysis (figure 13 | M,P). Primary OPCs were *A<sub>2</sub>B<sub>5</sub>*<sup>+</sup> and became *O4*<sup>+</sup> about 6-12h after plating. The first myelin producing cells appeared at d3 and about 45% of cells are MBP<sup>+</sup> at d4. Thus, morphology analysis and immunocyto stainings demonstrated primary OPCs to have the differentiation potential to form multipolar branched, myelinating oligodendrocytes.

Following OPC cell lines were tested for reproducibility of primary OPC differentiation potential and morphology experiments in order to reduce animal sacrifices and a faster realization of experiments.

### 5.1.2 Analysis of OPC cell line morphology

The OPC cell lines OLI-Neu and OLN-93 were chosen for morphology and differentiation potential analysis. After proliferation of cell lines in PLL coated T57 flasks with cultivation media, they were passaged and seeded into diverse media conditions to define an appropriate differentiation media. A reduction of serum is known to encourage primary OPC differentiation. Therefore, a serum percentage of 0.5 was used in all three tested differentiation media. The according cultivation media with a higher percentage of serum served as a control. One tested media contained 10 µg/ml of the *insulin like growth factor 1* (IGF1) because its binding to the IGF1 receptor play a vital role in oligodendrocyte development, survival and myelin genesis<sup>79,80</sup>. The Satos media already included 10µg/ml insulin. The media were changed every 2-3 days.

#### Media overview for OLN-93:

Satos media + 0.5% FCS  
DMEM + 0.5% FCS + IGF1  
DMEM + 0.5% FCS  
DMEM + 10% FCS (=cultivation media as a control)

#### Media overview for OLI-Neu:

Satos media + 0.5% HS  
DMEM + 0.5% HS + IGF1  
DMEM + 0.5% HS  
DMEM + 5% HS (=cultivation media as a control)

To identify the best differentiation media, d1-d4 OLN-93 and OLI-Neu cells were photographed (Olympus BX 71), immunocyto stained against maturation markers, lysed for protein expression analysis and compared.

When OLI-Neu cells were seeded in PLL coated flasks with media that either contained 5% or 0.5% horse serum (HS), a clear reduction of proliferation was obvious in every 0.5% HS containing flask. Independent of the used media (Satos or DMEM), 0.5% HS encouraged the OLI-Neu cells to form longer processes, a possible indicator for initiation of a differentiation process (figure 14 | C-H). However, the seeded cell number was important to obtain healthy looking as well as processing OLI-Neu cells and identified to be beneficial at 350 000 cells per T75 flask. When OLI-Neu and primary OPC morphologies were compared, there are visible differences in cell body appearance, number and type of processes and branching. Most of the OLI-Neu cells formed two to four processes that showed just slightly branching and therefore, were morphological comparable to primary OPCs until a pre-oligodendrocyte stage of differentiation. Further, within one flask two types of OLI-Neu cells were present, cells with small cell bodies and long processes and cells with wide cell bodies that did not necessarily form processes. Immunocyto stainings were performed to control differentiation status through developmental marker appearance.

Figure 1 consists of eight panels (A-H) showing fluorescence micrographs of HUVEC cells. The panels are arranged in a 4x2 grid. The left column (A, C, E, G) shows cells at day 1 (d1) and the right column (B, D, F, H) shows cells at day 3 (d3). The rows represent different media conditions: DMEM + 5% HS (A, B), DMEM + 0.5% HS (C, D), Sato's Media + 0.5% HS (E, F), and DMEM + 0.5% HS + IGF1 (G, H). The cells are stained with a fluorescent marker, likely DAPI, to visualize the nuclei. The images show the morphology of HUVEC cells under different conditions and time points.

44 | 74

#### **5.1.2.2 OLN-93 morphology in diverse media conditions**

Seeding of OLN-93 cells in PLL coated flasks with 0.5% fetal calf serum (FCS) resulted in a reduction of proliferation, independent of the used media (DMEM, Satos). Within the 10% FCS containing cultivation media, OLN-93 cells even grew above each other and tend to form grid-like structures (figure 14 | I-J) whereas in the 0.5% FCS containing media, the cells showed a high variation in morphology. Phenotypes of multiple or less, thick or thin processes that were highly or hardly branched with or without membranous structures were observed (figure 14 | K-P). Some OLN-93 cells in cultivation media showed multiple branched phenotypes too but the rapid proliferation rate seemed to prevent expansion and number of processes. A cell number of 250 000 cells per T57 flask was necessary to promote growth and process formation in media with 0.5% serum. Morphology analysis identified some OLN-93 cells to look comparable to primary OPCs at a bi- to multipolar stage. Nevertheless, most OLN-93 cells appeared like hybrids of type-II-astrocytes and oligodendrocytes as they showed wide and flat cell bodies with various branched processes. The diversity of OLN-93 cells within one flask complicated precise comparison and therefore, immunocyto stainings were performed to obtain more information about the expression of oligodendrocyte developmental makers.

Interestingly, both cell lines reacted with significant morphological alterations to serum reduction but remained unaffected by the kind of media (DMEM or Satos) or IGF1 addition. The tested differentiation media revealed no media composition to more or less support morphology alterations related to differentiation processes. Therefore, following immunocytochemistries were performed on cells grown in all potential differentiation media to identify the cell lines differentiation potential, the according cultivation media served as control.

#### **5.1.3 Analysis of morphology and differentiation potential with immunocytochemistry markers**

Established oligodendrocyte maturation markers were used to determine the developmental status of the OLI-Neu and OLN-93 cell lines. The differentiation potential of primary OPCs showed them to undergo maturation until fully differentiated, myelinating oligodendrocytes. Thereby, primary OPCs developed branched processes and became positive for the pre-oligodendrocyte marker O4. They extended in size and branching that resulted in myelin formation detected by the myelin basic protein marker MBP. According to those results, the cell lines were tested for reproducibility.

### 5.1.3.1 OLI-Neu cell line differentiation potential

OLI-Neu cells were positive for the oligodendrocyte marker O4 from d1 to d4 in all tested media conditions (figure 15). Therefore, OLI-Neu cells had the potential to represent a pre-oligodendrocyte developmental stage. In addition, morphology changes that indicated differentiation initiation were observed in all media with 0.5% serum (figure 15 | E-P). Those three differentiation media encouraged OLI-Neu cells to form long, slightly branched processes, whereas cells within the cultivation media showed wider cell bodies and less process formation but more membranous structures (figure 15 | A-D). The Satos media with 0.5% HS was identified to act most beneficial for a homologue cell population with about 70% of cells forming long processes. However, unlike OPCs, the OLI-Neu cells failed to extend in branching and never became positive for MBP in all tested media at d3 or d4.

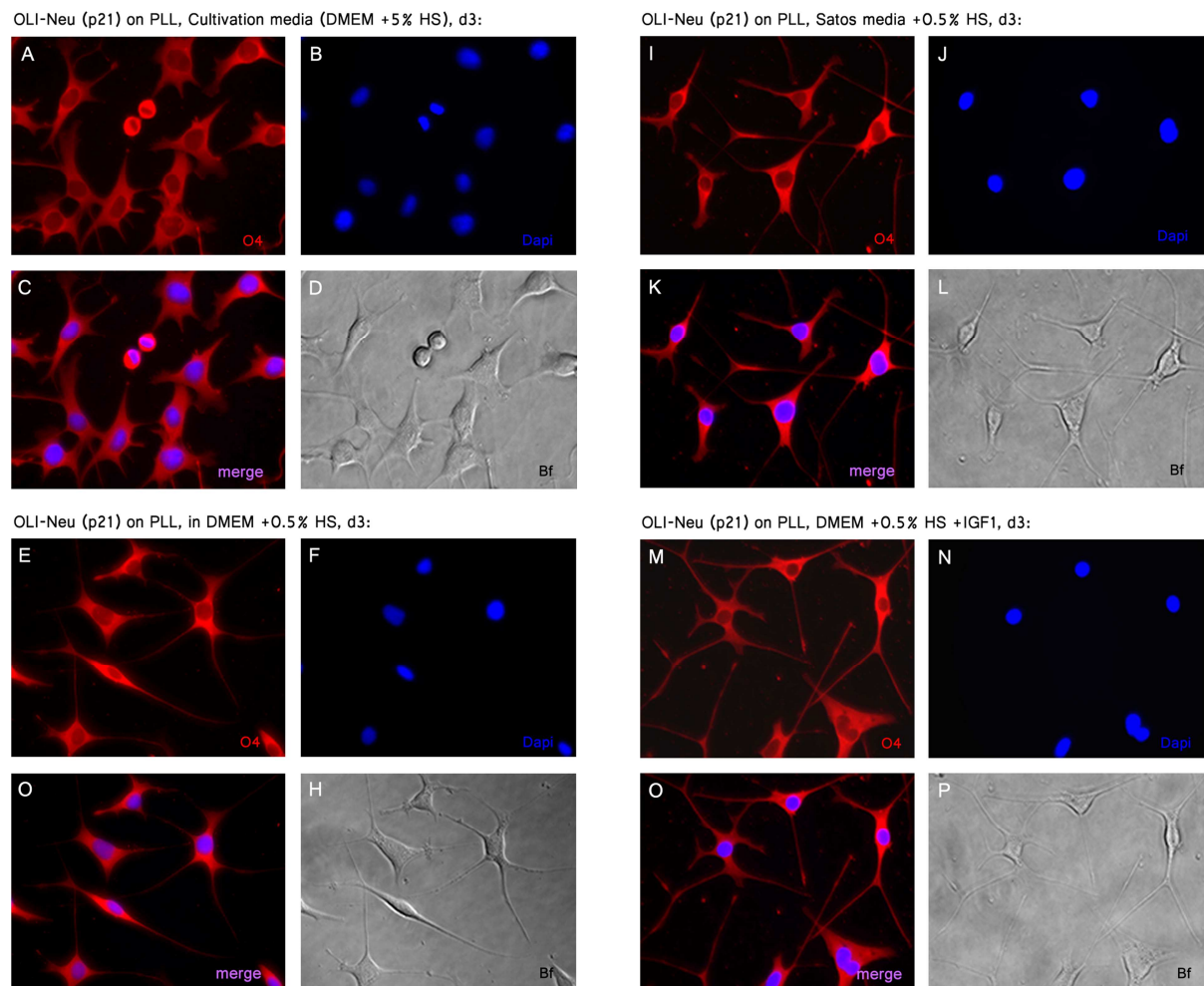


**Figure 15 | OLI-Neu cells in different media immunocyto stained against O4.** In all tested media, the OLI-Neu cells are equally positive for the marker O4. However, formation of long processes is predominant in media with 0.5% serum.



### 5.1.3.2 OLN-93 cell line differentiation potential

Independent of the used media, all OLN-93 cells were positive for O4 at d1 to d4 (figure 16). The three tested differentiation media promoted a branched, membranous phenotype but the kind of process formation highly varied within one flask. Most of OLN-93 cells were very flat and wide with membranous structures (e.g. figure 16 | M-P) or intensively branched (e.g. figure 16 | E-H) that indicated differentiation. Cells with thicker cell bodies and formation of long processes by less branching (e.g. figure 16 | I-L) were predominantly found in Satos media with 0.5% serum and comparable to primary OPCs at a bi- to multipolar stage. Following immunocyto stainings against MBP were negative suggesting OLN-93 cell line differentiation potential to end at a pre-oligodendrocyte stage of development. The morphological alterations to membranous, branched phenotypes therefore did not reflect a fully differentiated primary oligodendrocyte.

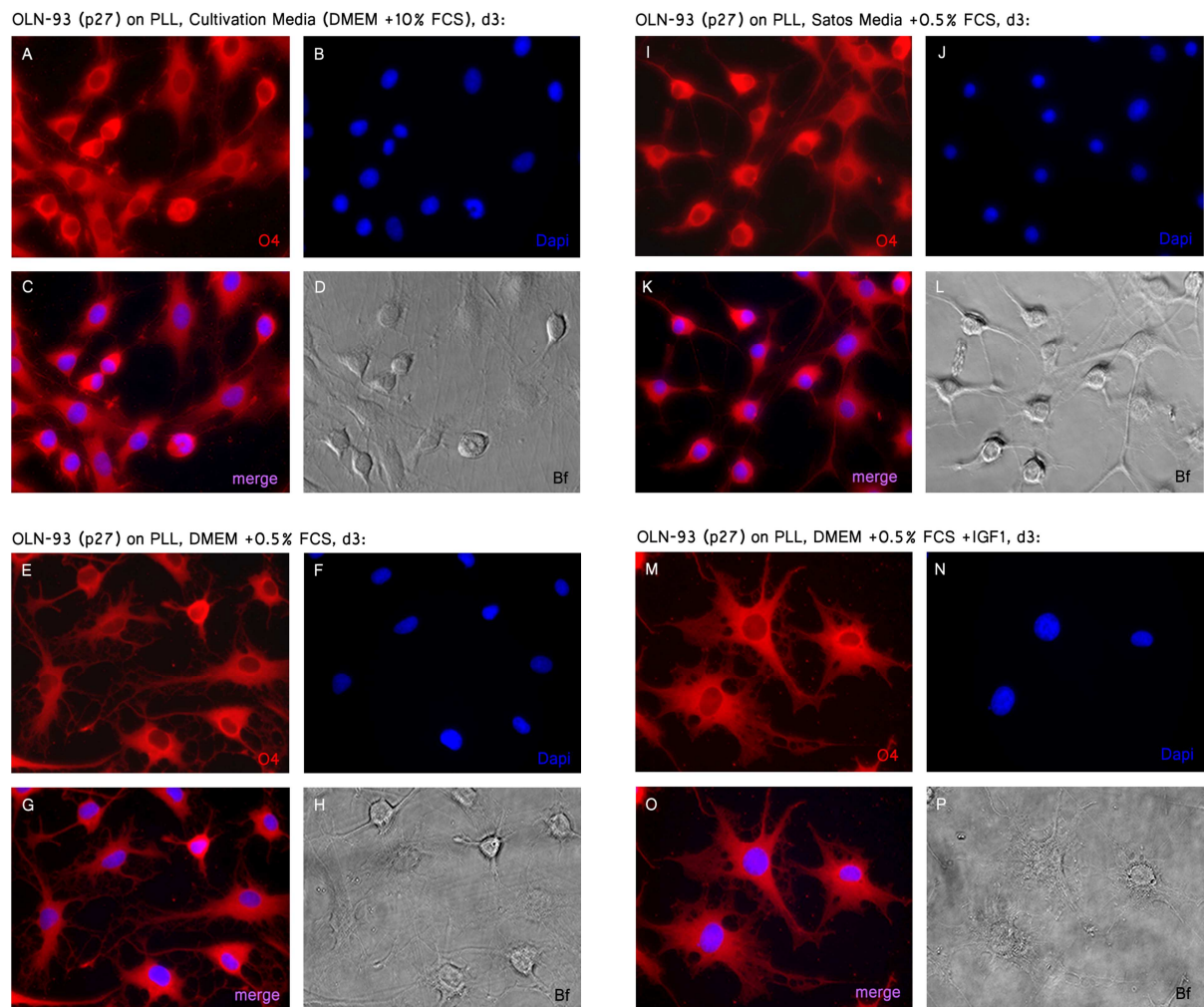


**Figure 16 | OLN-93 cells in different media immunostained against O4.** In all tested media, the OLN-93 cells are positive for the marker O4 but there is a high variability in cell morphology independent of the used media.

### 5.1.3.3 Morphological differences between primary OPCs and cell line cells

A closer look on morphological differences between primary OPCs and cell line cells was obtained through immunocyto stainings against the glial marker A<sub>2</sub>B<sub>5</sub>. Like primary oligodendrocytes both OLI-Neu and OLN-93 cells are positive for A<sub>2</sub>B<sub>5</sub> at d3 after cultivation in Satos media with 0.5% serum. However, when compared to primary oligodendrocytes, the cell lines display obvious morphological differences. OLI-Neu and OLN-93 cells showed bigger cell nuclei, wider cell bodies and different kinds of processes and branching at d3. (cp. figure 17)

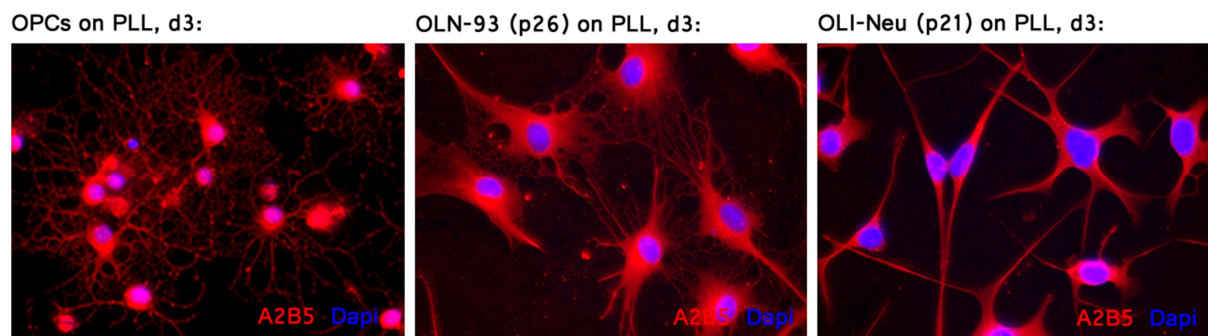


**Figure 17 | Morphology overview of primary oligodendrocytes, OLI-Neu and OLN-93 cells in Satos media + 0.5% serum.** All cells were positive for the glial marker A<sub>2</sub>B<sub>5</sub> but cell line cells showed significant morphological differences when compared to primary oligodendrocytes.

### 5.1.3.4 Morphological stages of OLI-Neu and primary OPC process formation

The differentiation of primary OPCs is subdivided in certain stages of process formation until a multipolar branched, myelinating phenotype is reached as illustrated in figure 18 | F-I. Morphology observations gave the impulse that the beginning OLI-Neu cells process formation could behave similar to primary OPCs even if an extensive branching was never reached.

Immunocyto stainings against O4 illustrated matchable morphological stages of OLI-Neu process formation until stage 2, a multipolar, slightly branched phenotype (figure 18 | A-D). In contrast to primary OPCs, all OLI-Neu cells were O4<sup>+</sup>. Even the most inhibited phenotype with no process formation was still positive for O4 and therefore counted for stage 0 (figure 18 | A). However, extensive branched OLI-Neu cells comparable to the stage 3 primary oligodendrocyte phenotype were never observed.

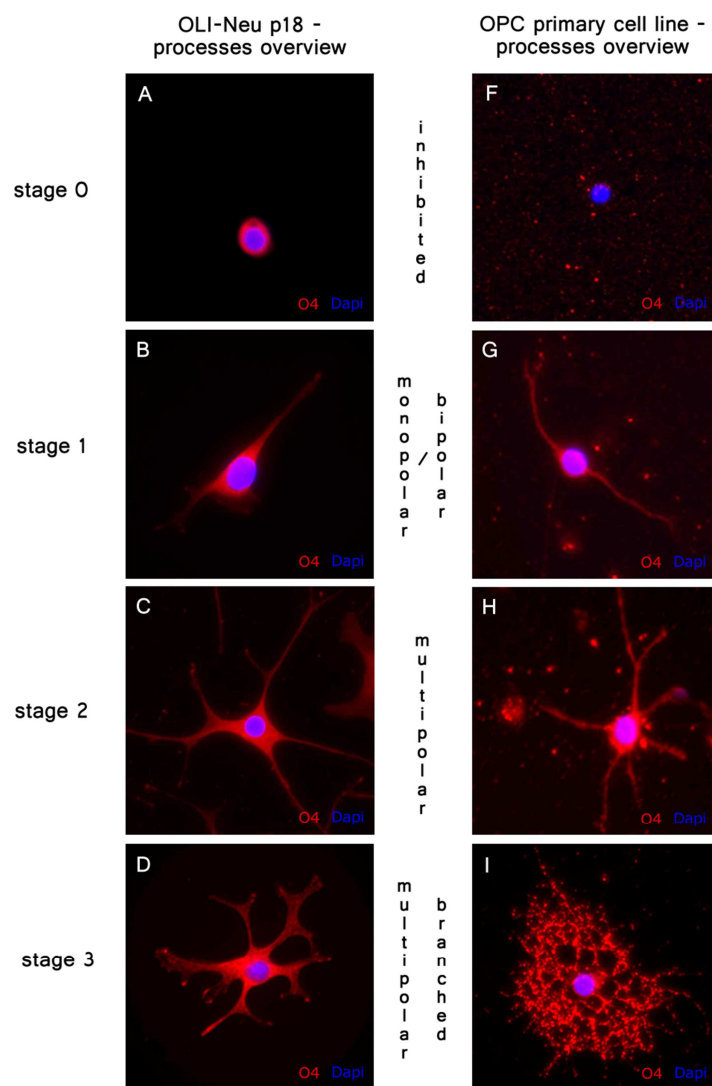


**Figure 18 | Morphological stages of OLI-Neu cells and OPCs.** F-I Stages of OPC process formation. It shall be noted, that OPCs without processes but positive for O4 are counted for stage 1. A-D Stages of OLI-Neu process formation.

#### **5.1.4 Analysis of the inhibitory potential of MPE and EphrinB3**

To calculate and compare the inhibitory potentials of MPE and IgG clustered EphrinB3 on primary OPCs, OLI-Neu and OLN-93, the cells were counted for presence in four defined morphological stages of development, whereas stage 0 = most inhibited phenotype and stage 3 = most differentiated phenotype. Thereby, at least 200 cells were counted from different wells cultivated in the particular condition (PLL, MPE, clustered EphrinB3) at d3. In every condition Santos media with 0.5% serum was used.

##### **5.1.4.3 OPCs on PLL**

When primary OPCs were seeded on PLL, about 45% differentiated into myelinating Oligodendrocytes (stage 3), 25% had multipolar processes that were slightly branched (stage 2) and about the same amount showed at least mono- or bipolar processes (stage 1). However, even in well differentiating conditions some OPCs did not form processes and were negative for O4 (stage 0). (cp. figure 20 | A)

##### **5.1.4.4 OPCs on MPE**

Upon seeding on MPE (40µg) coated dishes, OPC differentiation initiation was inhibited (figure 13 | L & O). Thereby, most OPCs hardly showed any process formation and about 75% were not even positive for the marker O4 at d1. They are still alive, displayed by an intense and well defined dapi staining (figure 19 | N) but in a quiescent stage. The remaining cells formed mono- to multipolar branched processes but never differentiated into myelinating oligodendrocytes. (cp. figure 20 | A)

##### **5.1.4.5 OLI-Neu cells on PLL**

At d3 after cultivation on PLL, 45% of OLI-Neu cells developed several long processes that were slightly branched (stage 2) whereas 15% also showed membranous structures (stage 3). At least 34% started to form mono- or bipolar processes (stage 1) and 5% showed no processes by being O4<sup>+</sup> (stage 0). (cp. figure 20 | B)

##### **5.1.4.4 OLI-Neu cells on MPE**

When OLI-Neu cells were seeded on dishes coated with 40µg MPE, 43% of OLI-Neu cells showed an inhibited phenotype with no process formation. A similar number of cells were found in a mono- or bipolar stage (figure 19 | F-J) and just about 15% formed multipolar, slightly branched but short processes. Interestingly, all inhibited cells were positive for the marker O4 (cp. figure 20) at d1. This fact demonstrated the OLI-Neu cells to represent an O4<sup>+</sup> developmental stage from the very beginning



but further differentiation was inhibited. However, less OLI-Neu cells were able to attach to MPE coated surfaces since they were found floating around dead in the media. (cp figure 20 | B)

#### 5.1.4.5 OLN-93 cells on MPE

In turn, OLN-93 cells remained completely unaffected when seeded on MPE coated dishes. Most of them formed multiple, branched processes and all were positive for O4 by having a good attachment rate (figure 19 | A-E). Therefore, no statistics were performed and OLN-93 cells were excluded for reproduction of the established primary OPC experiments.

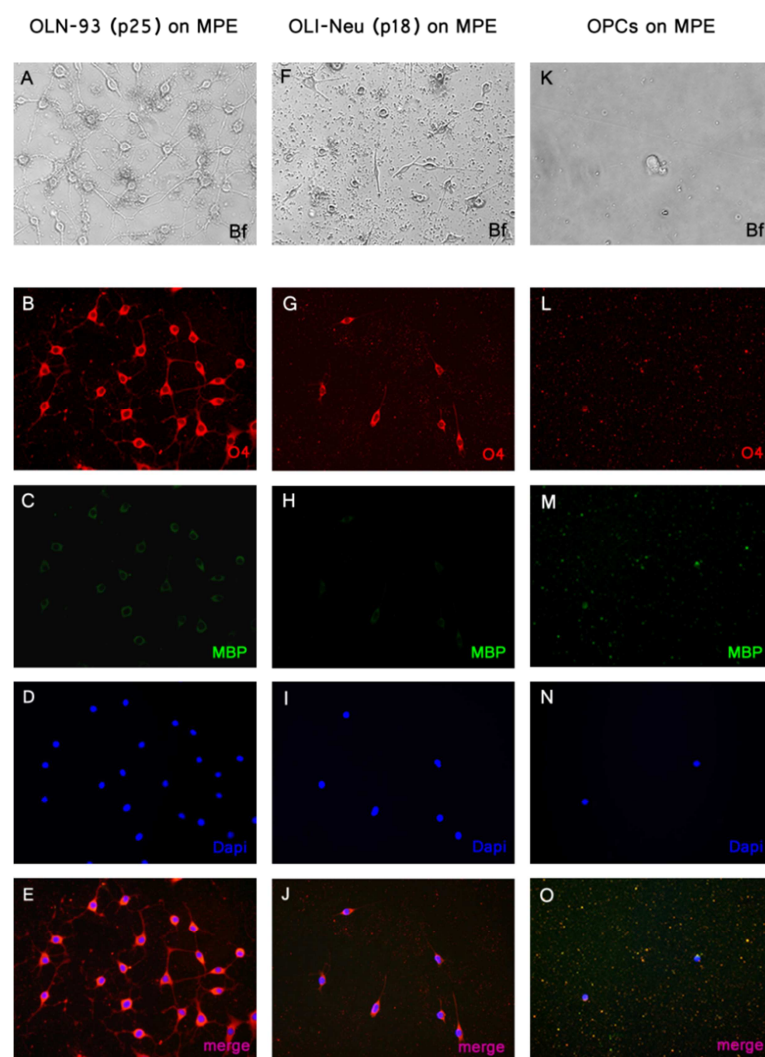


**Figure 19 | Primary OPCs and cell lines to MPE at d1.** K-O on MPE OPCs were strongly inhibited - no process formation and no expression of O4. F-J OLI-Neu cells hardly showed process formation on MPE but were O4 positive! A-E OLN-93 cells showed no significant inhibition on MPE and are O4 positive. C-M As expected, all cells were negative for MBP. Note the green appearing cells in C not to be MBP positive but just represent a strong background signal from the secondary antibody.

#### 5.1.4.6 Reaction of OPCs on EphrinB3

When inhibitor EphrinB3 (IgG clustered) was added 4h after seeding on PLL coated dishes, just 14% differentiated into myelinating oligodendrocytes and 21% remained in a pre- or immature oligodendrocyte phenotype. In contrast to MPE, OPCs showed no total inhibition upon EphrinB3 addition but 65% remained in an O4 positive, mono- or bipolar stage. This observation indicated EphrinB3 to inhibit predominantly the initiation of later differentiation processes. (cp. figure 20 | A)

#### 5.1.4.7 Reaction of OLI-Neu cells on EphrinB3

Addition of EphrinB3 4h after seeding caused OLI-Neu cells to react quite similar like primary OPCs. A minor percentage of OLI-Neu cells showed multipolar, slightly branched processes (17%) or enlarged membranous structures (9%). 40% of OLI-Neu cells were predominantly mono- or bipolar and 34% were O4 positive without process formation. (cp. figure 20 | B)

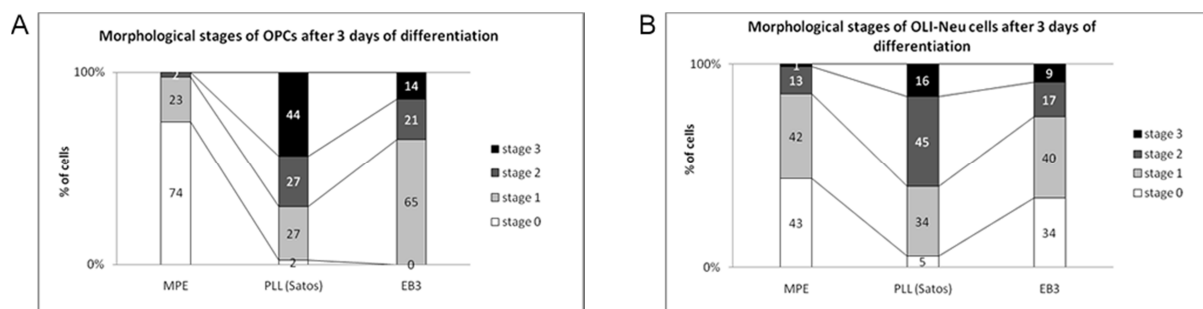


**Figure 20 | Morphological stages of OPC (A) and OLI-Neu (B) process formation in different conditions at d3.** The numbers of cells at four morphological stages were evaluated by counting of at least 200 cells in different wells according to condition (PLL, MPE, clustered EphrinB3) in Satos media, whereas stage 0 = most inhibited phenotype and stage 3 = most differentiated phenotype. Please note that just one well with OLI-Neu cells + Ephrin B3 was available for counting.

#### 5.1.5 Immunocyto staining results overview

Comparison of primary oligodendrocyte, OLI-Neu and OLN-93 cell lines immunocyto stainings (table 1) indicated OLI-Neu and OLN-93 cell lines to represent a pre-oligodendrocytal stage of development (O4 & A<sub>2</sub>B<sub>5</sub> positive) which, at least under the present conditions, could not be triggered further in the differentiation process until a MBP positive phenotype.

	Prim. Oligo.	OLI-Neu	OLN-93
O4 <sup>+</sup> on PLL (from d1)	98 %	100 %	100 %
O4 <sup>+</sup> on MPE (d1)	25%	100%	100%
O4 <sup>+</sup> with EphrinB3 (from d1)	100%	100%	-
MBP <sup>+</sup> on PLL (d3 to d4)	45%	0%	0%
MBP <sup>+</sup> on MPE (d1)	0%	0%	0%
A <sub>2</sub> B <sub>5</sub> <sup>+</sup> on PLL (from d1)	100%	100%	100%

**Table 1 | Overview of primary oligodendrocyte, OLI-Neu & OLN-93 cell line immunocyto stainings.**

## 5.2 Potential OPC-astrocyte switch

OPCs on PLL, Satos media, d7:

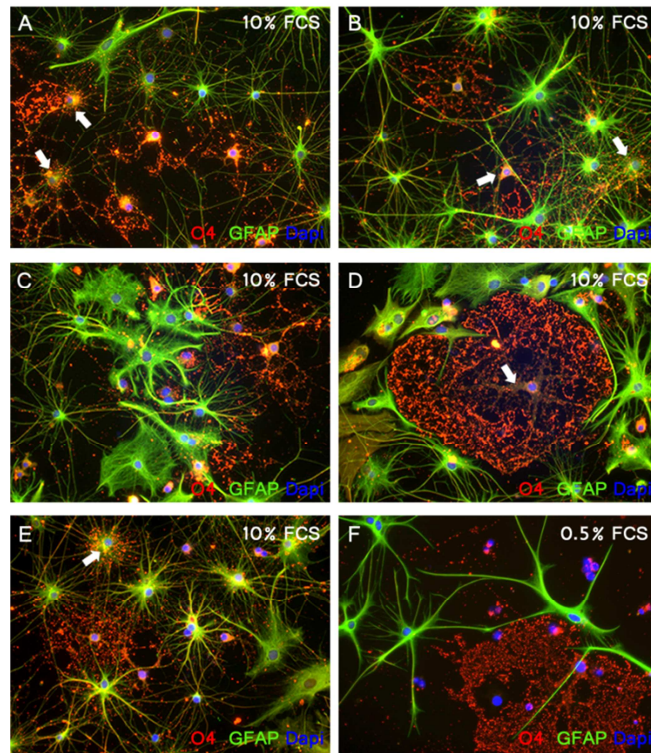


**Figure 21 | OPCs on PLL in Satos media with 10% FCS (A-E) or 0.5% FCS (F) at d7.** 10% FCS containing wells showed at least two different shaped types of astrocytes (GFAP<sup>+</sup> in green), Oligodendrocytes (O4<sup>+</sup> in red) as well as cells to be positive for both markers (most obvious ones indicated with white arrows).

a more compact cell body and multiple, astral processes) and in addition, some cells positive for both. Interestingly, those O4<sup>+</sup>/GFAP<sup>+</sup> cells looked like to have been originated from oligodendrocytes, which switched into an astrocyte phenotype (figure 21 | A-E white arrows). Even if this oligodendrocyte-type-II-astrocyte phenotype was just an *in vitro* relict, caused/promoted by an initial contamination from a bad shake off or a lack of nutrients, in Satos media with 0.5% FCS those O4<sup>+</sup>/GFAP<sup>+</sup> cells have never been observed. In addition, when astrocytes were present in media with 0.5% FCS (contamination normally less than 5%) they showed an astral like shape with thicker processes (figure 21 | F). The percentage of occurring cell types at d7 is illustrated in figure 22.

Primary OPCs were seeded in Satos media with either 0.5% or 10% FCS to illustrate morphological differences. After a change of media at d2 or d3, the cells were fixed at d7. Immunocytochemistry demonstrated oligodendrocytes positive for O4 and revealed several degrading myelin sheet structures (e.g. figure 21 | D). The degradation was thought to be due to the deprivation of nutrients. Surprisingly, the 10% FCS wells showed an unexpected high amount of cell types, not positive for O4. As it was very likely for those cells to be astrocytes, they were immunocytochemistry against the common astrocyte marker GFAP. The result displayed cells negative for O4 to be positive for GFAP and to appear in different shapes: type-I like astrocytes (wide and flat cells with no or less processes) or type-II like astrocytes (cells with

**Composition of cells in Satos media +10% FCS at d7**

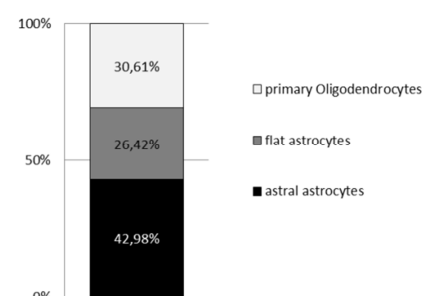


**Figure 22 | Percentages of present cell types in Satos media +10% FCS at d7.**

### 5.3 EM analysis of EphrinB3 KO mice

#### 5.3.1 Analysing of g-ratios

The g-ratios of CCP regions from 1M, 3M, 6M and old EphrinB3 KO and according control brains were evaluated at 6x magnification and compared. Thereby, about 20 axons with different diameters were analysed through calculation of the ratio between the inner axonal diameter divided by the total diameter (with myelin). The results showed this g-ratio to be very consistent in both general and when KO and control brains are compared as illustrated in figure 23.

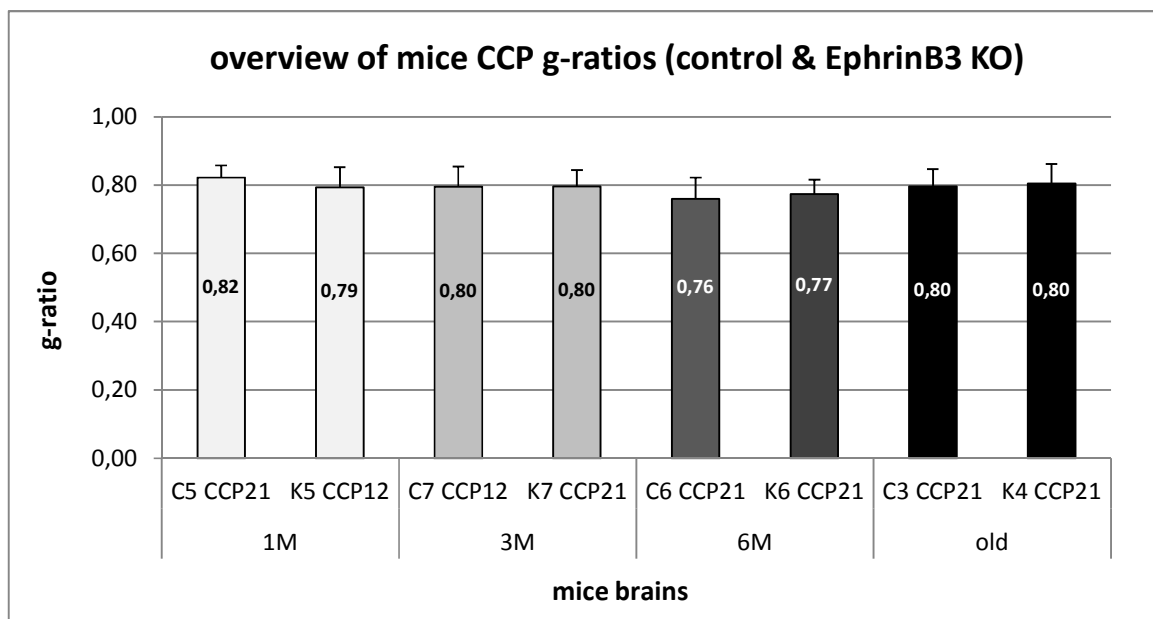
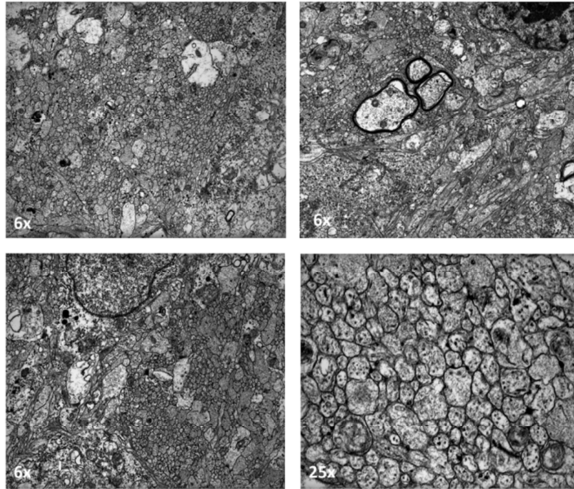


**Figure 23 | Overview of EphrinB3 KO and control CCP g-ratios.** EphrinB3 KO and control mice brains of different ages were evaluated for their g-ratios and compared, resulting in no significant changes.

#### 5.3.2 Differences in myelination

Analysing of knock out and control CCP brain regions through EM revealed differences in myelination appearances in d2 mice. Whereas the control brain showed hardly any axon myelination, the KO brain contained several regions of slight myelinated axons (figure 24 | d2 K2 CCP2 EM images). This observation could indicate that EphrinB3 KO promotes active myelination before postnatal day 6 (P6). In addition, former *in vitro* experiments confirmed EphrinB3 as an inhibitor of primary OPC differentiation and therefore, its knock out would match the result of prematurely myelination.

d2 K2 CCP2



d2 C2 CCP2

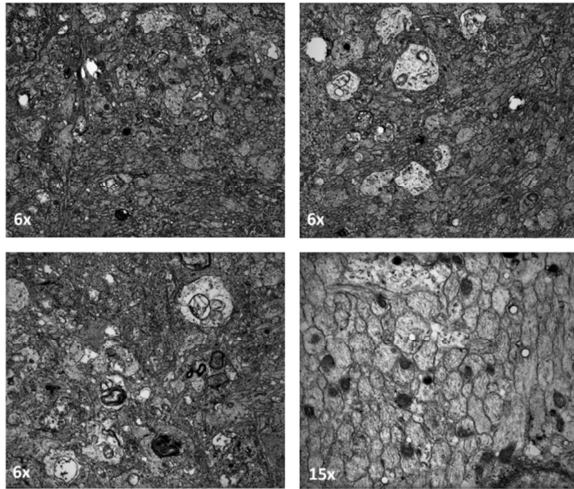
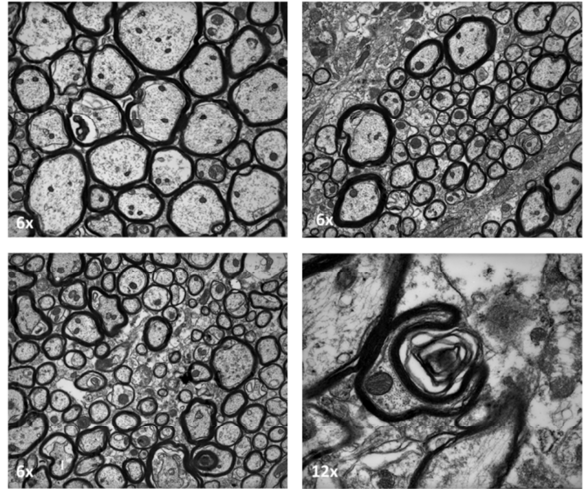


**Figure 24 | d2 K2 & C2 CCP EM images at different magnifications.** Note that d2 EphrinB3 KO EM images – in contrast to d2 controls – show several regions of slight myelinated axons!

1M K5 CCP12



1M C5 CCP12

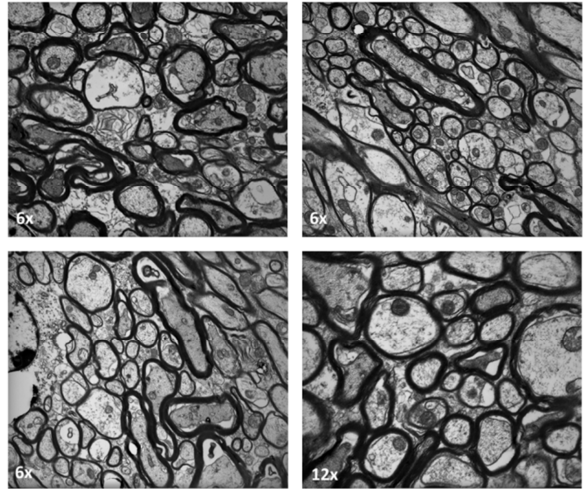
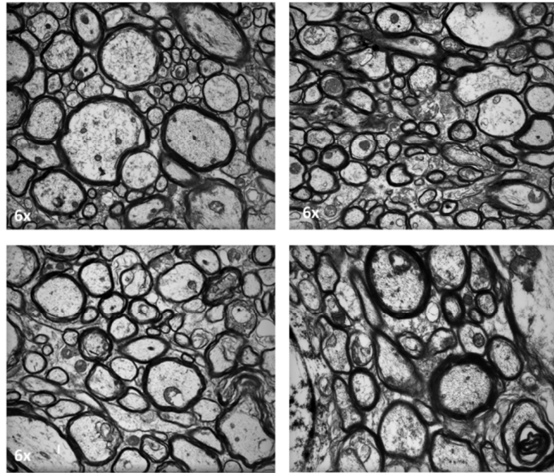


**Figure 25 | 1M K5 & C5 CCP EM images at different magnifications.**

The 1M (figure 25), 3M (figure 26), 6M (figure 27) and old (figure 28) KO and control CCP EM images exhibited no further obvious changes in myelination appearance. However, some animals were badly perfused (e.g. figure 27 | 6M C6 CCP21).



3M K7 CCP21



3M C7 CCP12

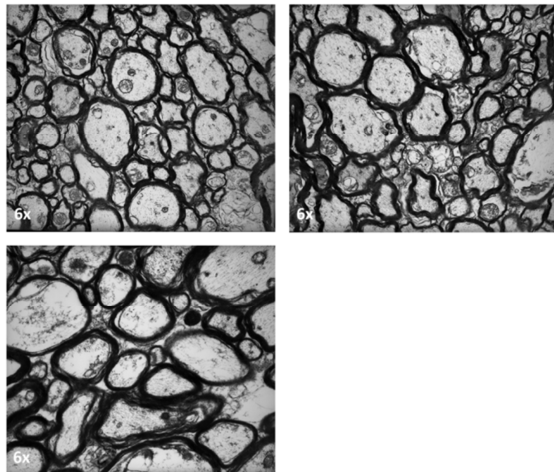
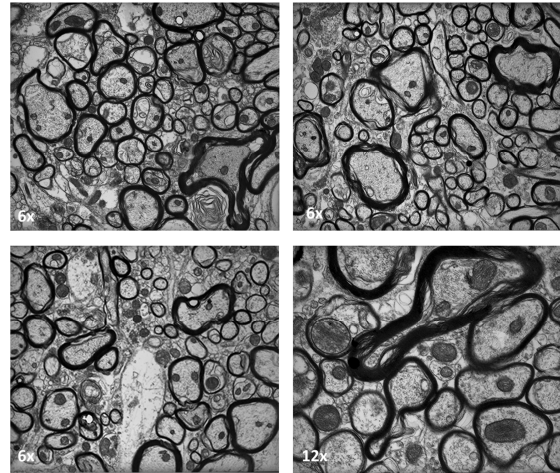


Figure 26 | 3M K7 & C7 CCP EM images at different magnifications.

6M K CCP21



6M C6 CCP21

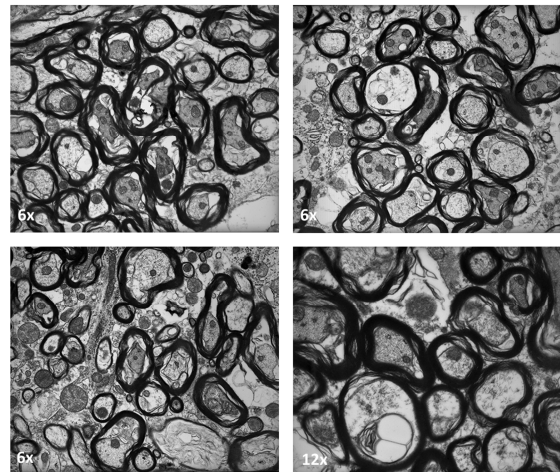
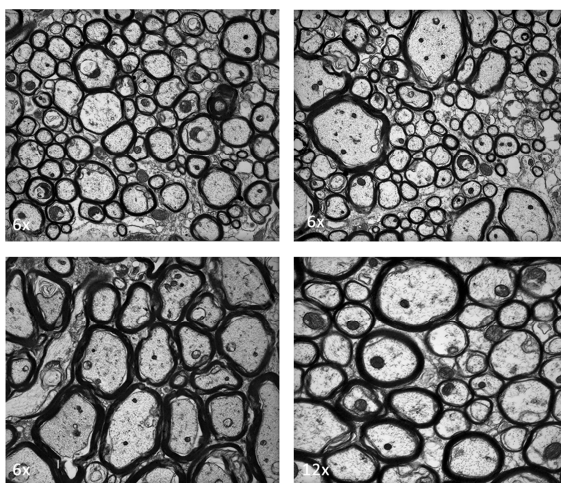


Figure 27 | 6M K6 & C6 CCP EM images at different magnifications. Note the bad animal perfusion in the control.

old K4 CCP21



old C3 CCP21

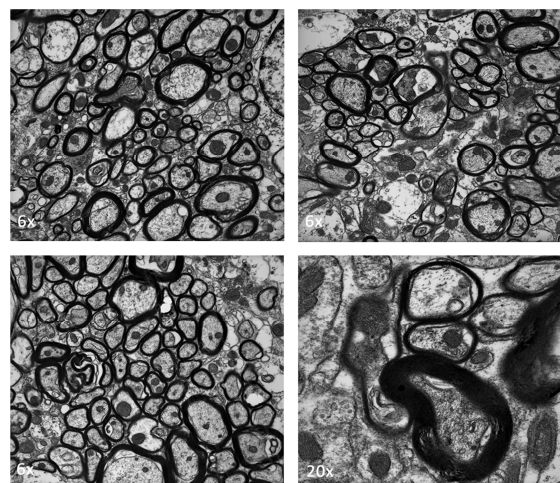


Figure 28 | old KO & control CCP EM images at different magnifications.

### 5.3.3 Myelin abnormalities

After different types of myelin abnormalities were identified and defined as ‘whatever’, ‘thick myelin wraps’, ‘multiple myelin wraps’, ‘multiple neuron wraps’, ‘messed up’, ‘infolding’ and ‘outfolding’, the EM specimen were evaluated for those myelin abnormalities without knowing if a control or KO specimen was watched (figure 29). The results illustrate an increased ‘whatever’ phenotype in the 1M EphrinB3 KO CCP and more ‘multiple myelin wraps’ in the 3M EphrinB3 KO compared to controls. However, no certain pattern of myelin abnormality occurrence was identified.

Myelin abnormalities - overview EphrinB3 KO & Control rat CCP

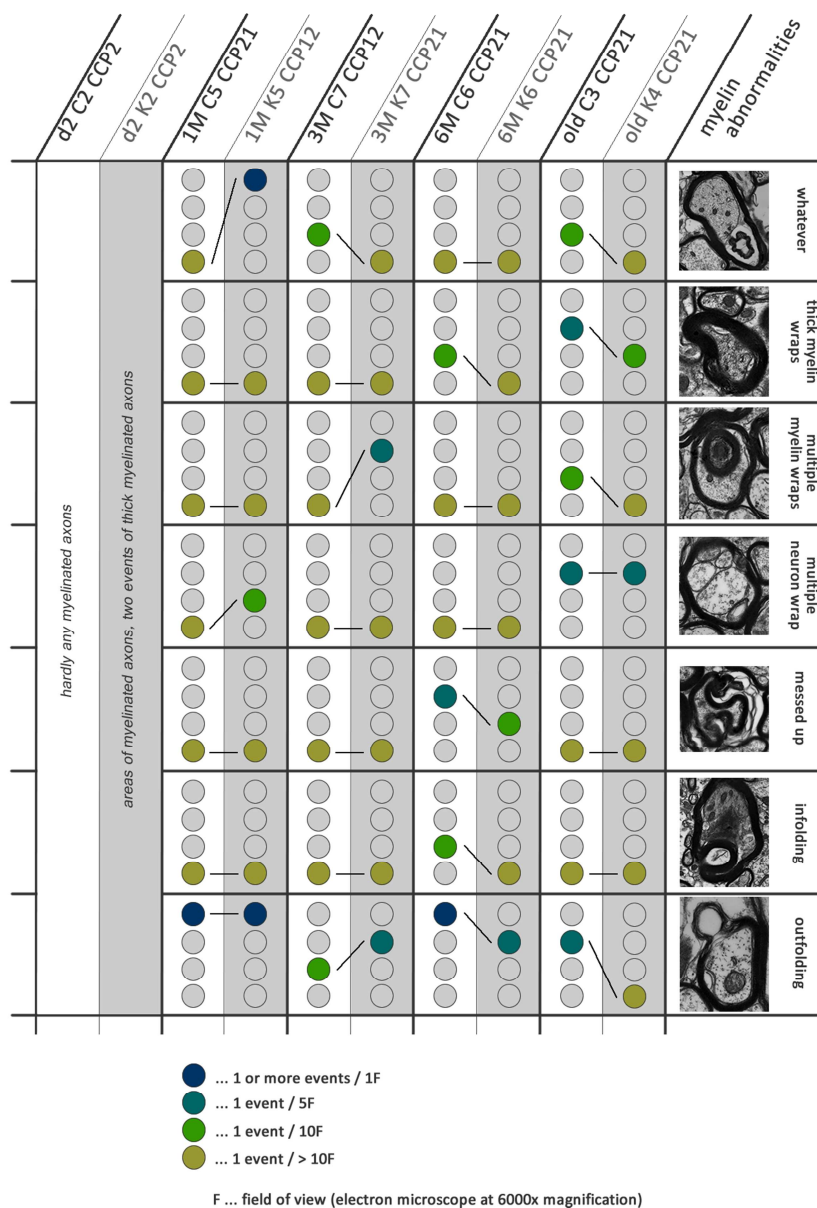


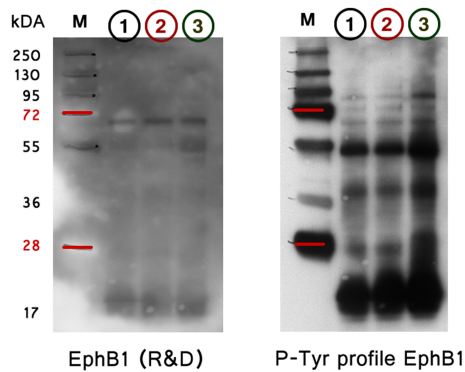
Figure 29 | Overview of myelin abnormalities in EphrinB3 KO and control CCP regions.

## 5.4 Analysing of EphrinB3 and its receptors

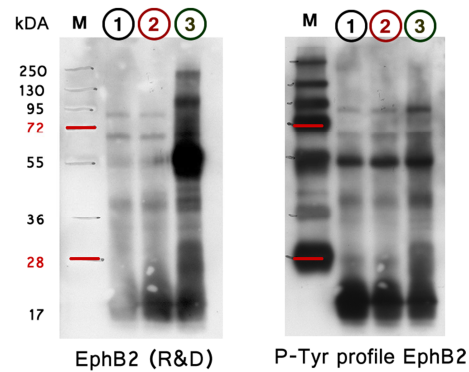
### 5.4.1 IP and phosphorylation analysis of Ephrin receptors

The immunoprecipitation of Eph receptors B1, B2, B3 and A4 were performed on primary OPCs either lysed at 45min or 4h after a settlement period of four hours. The results displayed the IP to probably fail since no receptor bands (about 110kDa) could be identified and a strong IP background band pattern complicated evaluation. The according phosphotyrosine profile exhibited also strong background bands and no clear interpretation could be obtained. Several other immunoprecipitations were performed with modified protocols but the assays (and according IP band patterns) pretty much reflect those in figure 30 | A-D.

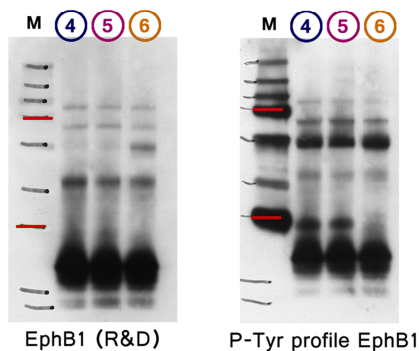
#### A EphB1 Phosphorylation Status Assay, 45min:



#### B EphB2 Phosphorylation Status Assay, 45min:



#### EphB1 Phosphorylation Status Assay, 4h:



#### EphB2 Phosphorylation Status Assay, 4h:

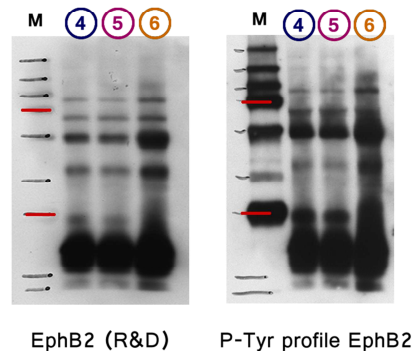
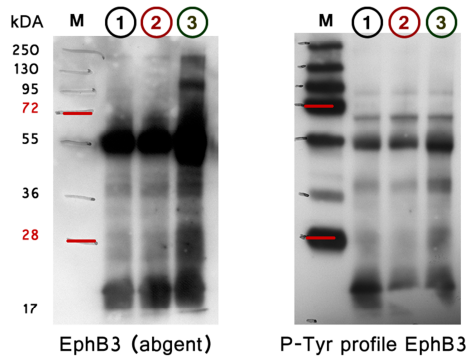


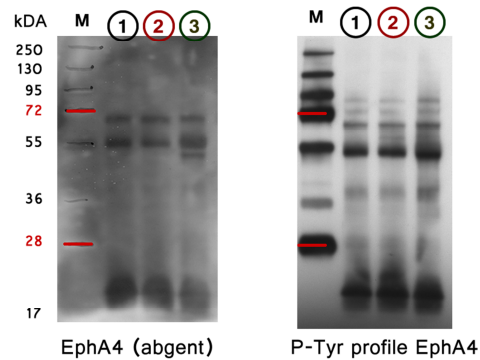
Figure 30 A-B | Overview of Phosphorylation Status Assays EphB1 (A) and EphB2 (B) at 45min and 4h after settlement period of OPCs.



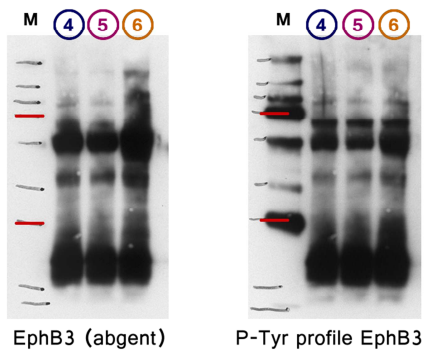
**C EphB3 Phosphorylation Status Assay, 45min:**



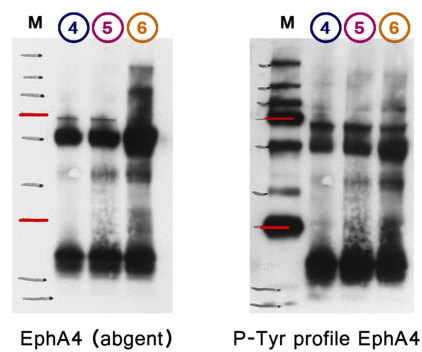
**D EphA4 Phosphorylation Status Assay, 45min:**



**EphB3 Phosphorylation Status Assay, 4h:**



**EphA4 Phosphorylation Status Assay, 4h:**



- ① ... OPC lysates, PLL, 45min, immunoprecipitated with according receptor antibody
- ② ... OPC lysates, EB3, 45min, immunoprecipitated with according receptor antibody
- ③ ... OPC lysates, PLL, 45min, immunoprecipitated with IgG (control)
- ④ ... OPC lysates, PLL, 4h, immunoprecipitated with according receptor antibody
- ⑤ ... OPC lysates, EB3, 4h, immunoprecipitated with according receptor antibody
- ⑥ ... OPC lysates, PLL, 4h, immunoprecipitated with IgG (control)

**Figure 30 C-D | Overview of Phosphorylation Status Assays EphB3 (C) and EphA4 (D) at 45min and 4h after settlement period of OPCs.**

### 5.4.2 IP of Eph receptors

In this study, several immunoprecipitations were performed on Eph receptors B1, B2, B3 & A4 but distinct bands could never been identified. Further experiments were needed to ensure the Eph receptors were not precipitated during lysate preparation. Therefore, oligodendrocyte d2 lysates were centrifuged and 30 µg of the supernatant and the whole according pellet were loaded on a SDS gel. SDS-page was followed by western blotting to detect all four Eph receptors. The result (shown in figure

Eph-Receptor detection out of OPC lysates (supernatant & pellet)

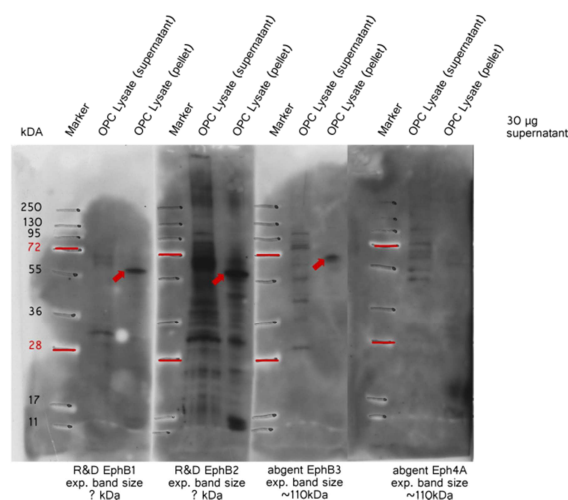


**Figure 31 | OCP lysate supernatants and pellets detected against Eph receptors B1, B2, B3 and A4.** Eph receptor bands are expected at about 110 kDa.

31) displayed several bands in the supernatant lines but hardly and very slight at the right weight (e.g. for Eph receptors B3 and A4 at about 110 kDa). In addition, R&D gave no information at which weight Eph receptors B1 and B2 bands should be expected. Interestingly, in the pellet lanes detected against Eph receptors B1 and B2 very strong bands about 60 kDa and against Eph receptor B3 a clear band about 70 kDa appeared (red arrows). Those could indicate that the receptors were not proper dissolved from the cell membranes and therefore precipitated in the pellet. However, if this is the case their detected band sizes did not correspond to the expected ones.

### 5.4.3 IP of EphrinB3 out of MPE

The immunoprecipitation of EphrinB3 out of MPE failed several times and was thought to be due to the precipitated detergent Octyl β-D-pyranoglycoside. Therefore, the MPE was centrifuged two times at 8000 rpm for 3 min to obtain a clear supernatant (=supernatant2). The following IPs on supernatant2 were either performed with the EphrinB3 antibody from abcam or R&D. In addition, one probe of a brain lysate was available for analysis. After centrifugation to obtain a quiet clear supernatant the IP was performed with the more trusted abgent EphrinB3 antibody and the pellet served as a control. Other controls were 1) the pellet after first MPE centrifugation as EphrinB3 was possible precipitated, 2) pure MPE (0.8 mg/ml), 3) supernatant2 immunoprecipitated with IgG and 4) 'immunoprecipitated' 1x PBS to identify the IP band pattern.

When the IP was realized with the abcam EphrinB3 antibody, EphrinB3 was detected with the R&D EphrinB3 antibody and vice versa. The EphrinB3 band was expected either at about 36 kDa (abcam datasheet) or about 58 kDa<sup>90</sup>. However, a strong band was just observed in the brain lysate lane (figure

32 A | upper band in the big red circle) immunoprecipitated with the abcam EphrinB3 antibody. However, the IgG control lane contained a slighter but comparable band at the same high (figure 27 A | band in the small red circle). This result indicated the presumable EphrinB3 band either to be hidden by the IP band pattern or to be a part of the IP band pattern.

IP with the R&D EphrinB3 antibody (figure 32 | B) showed no bands at the expected high and the IP band pattern (c.f. 1x PBS and IgG lane) was equivalent to the band of supernatant2 immunoprecipitated with R&D EphrinB3 antibody. Nevertheless, both EphrinB3 antibodies detected no bands in the pure MPE or pellet lanes.

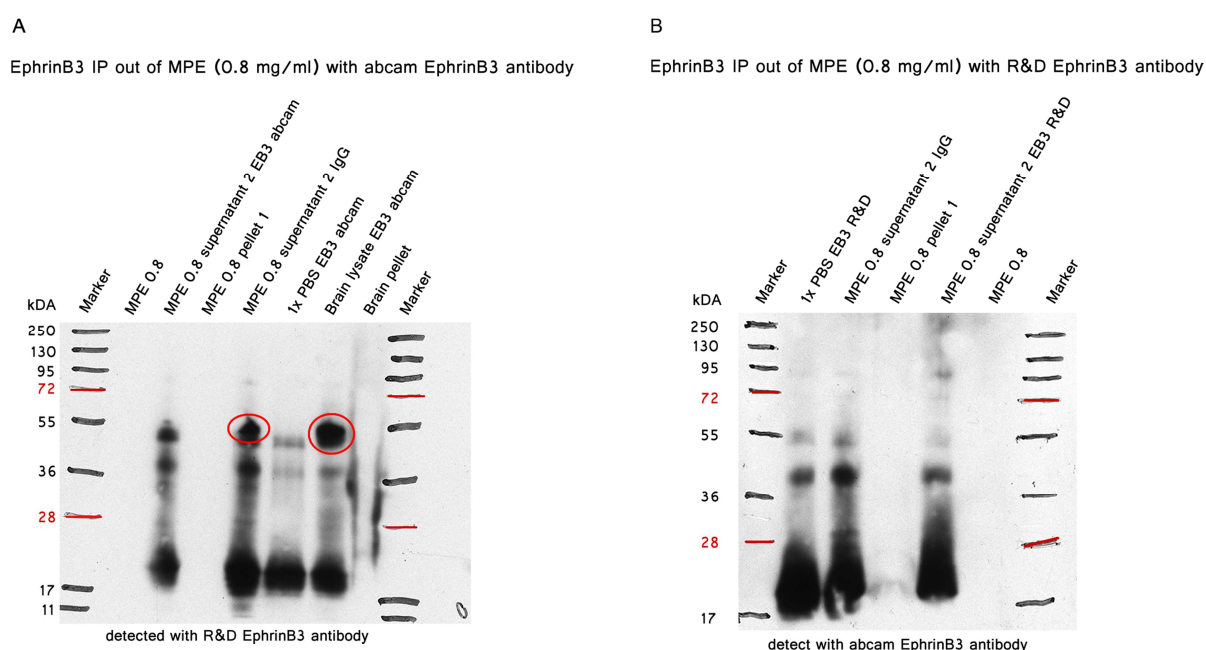


**Figure 32 | EphrinB3 immunoprecipitations with either abcam EB3 (A) or R&D (B) EB3 antibody**

It shall be noted that the illustrated IP band pattern in figure 32 was comparable to those of former experiments, even when different lyse or wash buffers were used.

#### 5.4.4 IP of EphrinB3 out of primary oligodendrocyte lysates

Here, EphrinB3 was tried to be immunoprecipitated out of primary oligodendrocyte lysates at different stages of development (day 0, day 1, day 2). As it was still not clear whether EphrinB3 is precipitated during lysate preparation, the corresponding pellets served as controls. To visualize the IP band pattern 'immunoprecipitated' 1x PBS was used. The IPs in this experiment were performed with the R&D EphrinB3 antibody.

Ephrin B3 immunoprecipitation out of OPC lysates with R&D EB3 antibody

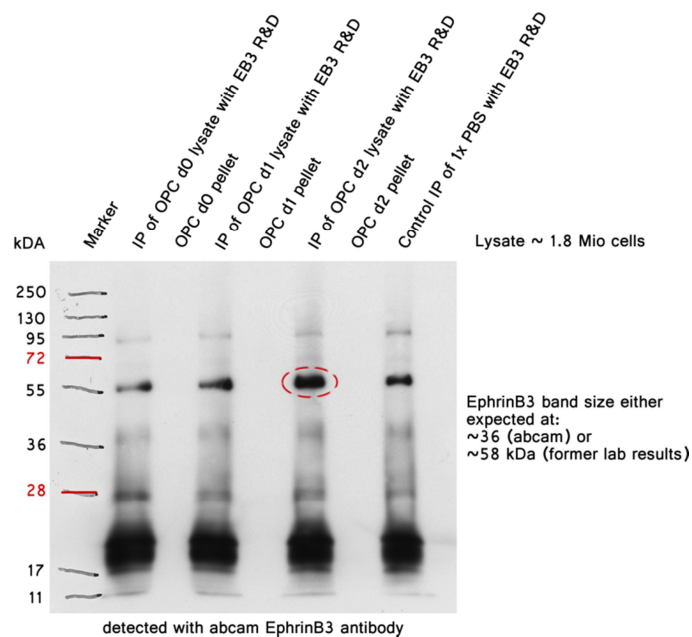


**Figure 33 | Immunoprecipitation of EphrinB3 out of primary oligodendrocyte lysates from different developmental stages.** (d0 = 8h after seeding, d1 = pre-oligodendrocytes, d2 = mostly immature oligodendrocytes)

The results displayed all band patterns to resemble those of the 1x PBS control. Nevertheless, there was a slightly thicker band about 55kDa in the oligodendrocyte d2 lysate line (figure 33 | red circle) whereas the IP band pattern showed the same intensity like the others. This could, according to the former result in 4.4.3) indicate the presumable EphrinB3 band either to be hidden by the IP band pattern or to be a part of the IP band pattern.

## Conclusion & Discussion

Established OPC experiments were repeated and confirmed

OLN-93 and OLI-Neu cell lines are not suitable to reproduce OPC experiments

Potential oligodendrocyte astrocyte switch *in vitro* with 10% FCS

Day2 EphrinB3 KO mice CCPs showed differences in myelination

Immunoprecipitation of Eph receptors B1, B2, B3 & A4 and EphrinB3 probably failed

## 6. Discussion

### 6.1 Primary OPCs versus cell lines

#### 6.1.1 Primary OPC experiments

In this study, I could repeat and confirm methods such as the purification of primary oligodendrocytes out of P0-P2 rat brains and the preparation of *myelin protein extracts* (MPE) out of adult rat brains to realize following OPC experiments. Differentiation and inhibitory studies were performed by analysing primary oligodendrocyte morphology changes and immunocytochemistry marker expression. Whereas differentiation studies demonstrated primary OPCs to have the differentiation potential to develop into myelinating oligodendrocytes, inhibitory studies displayed primary OPCs lineage progression to be inhibited by MPE and EphrinB3. Thereby, MPE acts predominantly on the very beginning of OPC differentiation as most of the cells remained in a quiescent, O4 negative stage. In contrast, the inhibitory potential of EphrinB3 prevents the initiation of differentiation processes after O4 expression.

Those results displayed the basic requirements the OPC cell lines OLI-Neu and OLN-93 need to be able to reproduce in order to reduce animal sacrifices and a faster realization of experiments.

#### 6.1.2 Analysis of OPC cell line OLN-93 displayed them to be not

First morphology analysis showed most OLN-93 cells to form differentiated-like phenotypes upon serum reduction to 0.5% at d3. Those cells appeared very flat and wide with membranous structures or intensively branched thought to indicate an on-going differentiation process. Although those phenotypes were different to primary OPCs after the same time of development, they were possible to represent an altered kind of differentiation. However, at some regions cells with thicker but small cell bodies that formed long, fine and less branched processes were observed. Those were comparable to primary OPCs at a bi- to multipolar stage and thought to be not fully differentiated.

Following immunocytostainings revealed OLN-93 cells to be positive for the glial cell marker A<sub>2</sub>B<sub>5</sub> and the pre-oligodendrocyte marker O4 but they failed to become positive for the myelin marker MBP suggesting the OLN-93 cell line differentiation potential to end at a pre-oligodendrocyte stage of development. Therefore, the observed morphological alterations to membranous, branched phenotypes of OLN-93 cells did not reflect a fully differentiated primary oligodendrocyte.

In addition, OLN-93 cells remained unaffected by MPE, a potent inhibitor of primary OPCs differentiation initiation. Thus, it is very likely that the OLN-93 differentiated-like phenotypes were in vitro relicts that did not longer represent the original OPC characteristics. In turn, the smaller, bi- to multipolar processed OLN-93 cells probably represented the original cell line cells.

According to those results, a recent publication revealed the morphological changes of OLN-93 cells to not reflect biochemical and functional differentiation. Further, just quiet high passage numbers of OLN-93 cells were available for this study (>24) and the same publication strongly recommends to use passage numbers <10 as over sub-culturing dramatically changed the cell line properties. This could explain the diversity of OLN-93 cells that appeared within one flask. Finally, it was declared that morphology changes not necessarily represent on-going differentiation processes and that serum conditions can easily alter cell type appearances.<sup>82</sup>

### 6.1.3 OLI-Neu cells

Analysis of OLI-Neu cells revealed morphology changes that could indicate a differentiation initiation process as upon serum reduction to 0.5%, the OLI-Neu cells formed several long, slightly branches processes at d3. However, no further signs of differentiation such as extensive branching or myelin-like structures were observed.

Positive immunocyto stainings against A<sub>2</sub>B<sub>5</sub> and O4 displayed matchable morphological stages of OLI-Neu and primary OPC process formation until a multipolar, slightly branched phenotype. However, OLI-Neu cells failed to become MBP positive indicating the cells to represent a pre-oligodendrocyte stage of development, confirmed by a publication from EM Krämer & T Koch in 1997.<sup>83</sup>

Inhibitory experiments with MPE showed OLI-Neu cells to be inhibited since they formed less and shorter processes. Interestingly, even the most inhibited phenotype with no processes was still positive for O4. This fact revealed the OLI-Neu cells to probably display an O4<sup>+</sup> developmental stage from the very beginning. Further, the inhibitory potential of EphrinB3 on OLI-Neu cells was illustrated to be comparable to primary OPCs.

Altogether, differentiation and inhibitors studies showed early OLI-Neu passages usable to study OPC differentiation events until a multipolar, slightly branched phenotype. However, they were not suitable for developmental studies as they never reached a myelinating phenotype.

### 6.1.4 Summary

Analysis of morphology and immunocytochemistry marker expression revealed the OLI-Neu and OLN-93 cell lines to represent oligodendrocytal cells arrested in an O4 positive stage of differentiation. In contrast to OPCs, they did not have the potential to progress in development since at least under the tested conditions no myelinating phenotype was observed. Thus, the OLI-Neu and OLN-93 cell lines are not suitable to reflect primary OPC differentiation into myelinating phenotypes. It shall always be remembered that cell lines are immortal due to certain mutations and tend to alter their original characteristics upon a few passages. They represent one certain type of cell and may not share the potential to progress in development.

## 6.2 Potential oligodendrocyte-astrocyte switch *in vitro* with 10% FCS

It was established a while ago that OPCs develop into astrocytes or oligodendrocytes depending on the used serum percentage. Serum rich media about 10% FCS promotes type-II-astrocyte development whereas 0.5% FCS leads to oligodendrocyte development.<sup>4</sup> To illustrate those morphological differences, primary OPCs were seeded in Satos media with either 0.5% or 10% FCS. The media was changed at d2 or d3 and the cells were fixed at d7. However the cells should have been fixed at d4, immunocyto stainings against the pre-oligodendrocyte marker O4 and the astrocyte marker GFAP confirmed the former statement. In the 10% FCS containing wells, the 43% of OPCs developed into GFAP<sup>+</sup>, astral shaped type-II-astrocytes and 31% showed O4<sup>+</sup> oligodendrocytes, predominantly at a pre- to immature differentiation stage. Interestingly, about 26% of cells displayed a GFAP<sup>+</sup>, wide and flat type-I-astrocyte phenotype that Raff & Miller (1983) did not report. In addition, some cells were positive for both O4 and GFAP and in the first place were counted GFAP<sup>+</sup>. Interestingly, about 25% of GFAP<sup>+</sup> cells looked like to have been originated from oligodendrocytes which switched into an astrocyte phenotype by forming multiple, long and fine GFAP<sup>+</sup> astral processes but they were O4<sup>+</sup> around and at the cell body. Even if those O4<sup>+</sup>/GFAP<sup>+</sup> cells were just *in vitro* artefacts caused by an initial contamination from a bad shake off or a lack of nutrients, in Satos media with 0.5% FCS those O4<sup>+</sup>/GFAP<sup>+</sup> cells have never been observed. In addition, when astrocytes were present in media with 0.5% FCS (contamination normally less than 5%) they showed less and thicker astral processes. However, it is comprehensible that GFAP<sup>+</sup>/O4<sup>+</sup> cells are just aberrant cells induced by culture conditions. Even if this oligodendrocyte-astrocyte switch exists, it is very unlikely to represent a normal stage of development and this observation just discloses the tight developmental relationship between astrocytes and oligodendrocytes.

## 6.3 Day 2 EphrinB3 KO mice showed a premature beginning of active myelination

Evaluation of 1M, 3M, 6M and old EphrinB3 KO and control mice EM images of CCP regions showed very consistent g-ratios when compared to the according control. In addition, the average of all g-ratios together was determined to be 0.79 that matched the normal CNS g-ratio of 0.7.<sup>50</sup>

To investigate whether the EphrinB3 KO caused myelin abnormalities, phenotypes were defined and counted for of their frequency of occurrence. The result revealed myelin abnormalities to occur independent of EphrinB3 KO or age.

When EM tissue samples of d2 EphrinB3 KO and d2 control brains were analysed, the EphrinB3 KO CCP areas revealed several regions of slight myelinated axons whereas the controls hardly showed any myelination. The 1M, 3M, 6M and old KO and according control specimen exhibited no obvious



differences in myelination. This indicated that EphrinB3 KO promoted active myelination before the normal beginning at postnatal day 6 (P6)<sup>84</sup> but thereby, did not affect the correct development of myelin. According to this finding, former *in vitro* experiments identified EphrinB3 as a potent inhibitor of OPC differentiation.<sup>78</sup> Therefore, its knock out is plausible to cause prematurely myelination. This finding is for sure the most important result in this study. However, this experiment was only performed at once and is strongly recommended to be repeated. The facts that EphrinB3 knock-out mice already exist and phenotypes are presumably obtained in P0 to P18 mice will cause just minor costs of animal keeping but could reveal important new insights of EphrinB3 and its impact on myelination *in vivo*.

## 6.4 EphrinB3 and its receptors Eph B1, B2, B3 & A4

### 6.4.1 Eph receptors B1, B2, B3 & A4 were probably precipitated with cell membrane debris

Several immunoprecipitations (IPs) on Eph receptors B1, B2, B3 & A4 were performed out primary oligodendrocytes lysates without identification of distinct bands. The reason was thought to be either an incomplete dissociation from the oligodendrocyte cellular membrane or a problem within the IP procedure. Eph receptor IPs were shown to work in the lab before, therefore, the problem seemed rather to be due to the handling than the method itself. Nevertheless, the possibility of precipitated Eph receptors together with cell membrane debris after primary oligodendrocyte lysate centrifugation was verified by loading of these pellets on a SDS-Page together with the according supernatant in the neighbouring lane and following detection for specific Eph receptor. The results displayed several bands in the supernatant lanes but hardly and if just very slight at the right weight of about 110 kDa. Interestingly, in the pellet lanes of Eph receptors B1, B2 & B3 very strong bands appeared that could indicate the receptors to be not totally dissolved from the cell membranes. However, if this is the case their detected band sizes did not correspond to the expected one and thus, it is still not clear whether the bands just display fragments of Eph receptors or whole Eph receptors.

### 6.4.2 EphrinB3 probably failed

Detection of EphrinB3 after IPs out of MPE, primary oligodendrocyte lysates or brain lysate displayed strong IP band patterns that looked quite similar to PBS controls in all experiments. However, a strong band could be observed in the brain lysate lane (immunoprecipitated with the abcam EphrinB3 antibody) and in the OPC d2 lysate lane (immunoprecipitated with the R&D EphrinB3 antibody) at about 55 kDa. EphrinB3 is expected either at about 36 kDa (abcam datasheet) or about 58 kDa<sup>90</sup> and therefore, it is possible that the bands displayed EphrinB3. Nevertheless, those results gave no clear information whether the presumable EphrinB3 band is hidden by or part of the IP band pattern.

## 7. References

1. Virchow R (1846) Über das granulierte Aussehen der Wandungen der Gehirnvventrikel. *Allg Z Psychiat* 3:242-250.
2. Kettenmann H, Ransom BR. *Neuroglia*. xix. Oxford University Press; New York: 2005. p. 601pp.
3. Richardson WD, Kessaris N & Pringle N (2006) Oligodendrocyte wars. *Nature Reviews Neuroscience* 7, 11-18 doi:10.1038/nrn1826.
4. Raff MC & Miller RH (1983). A glial progenitor cell that develops in vitro into an astrocyte or an oligodendrocyte depending on culture medium. *Nature*, Jun 303:390-396.
5. Nunes MC, Roy NS, Keyoung HM, Goodman RR, McKhann G, Jiang L, Kang J, Nedergaard M, Goldman SA (2003). Identification and isolation of multipotential neural progenitor cells from the subcortical whitematter of the adult human brain. *Nat. Med.* 9: 439–447.
6. Temple S (2001). The development of neural stem cells. *Nature* 414, 112–117
7. Temple S & Raff M (1986). Clonal analysis of oligodendrocyte development in culture: evidence for a developmental clock that counts cell divisions. *Cell* 44: 773-779
8. Sarlieve LL, Fabre M, Susz J and Matthieu JM (1983). Investigation on myelination in vitro. IV. 'myelin-like' or premyelin structures on cultures of dissociated brain cells from 14 to 15 day old embryonic mice. *Neurosci Res* 10: 191-210.
9. Matsuda Y, Koito H and Yamamoto H (1997). Induction of myelin-associated glycoprotein expression through neuron-oligodendrocyte contact. *Dev. Brain Res* 100: 110-116.
10. Warf BC, Fok-Seang J and Miller RH (1991). Evidence for the ventral origin of oligodendrocyte precursors in the rat spinal cord. *J. Neurosci.* 11: 2477–2488.
11. Fogarty M, Richardson WD and Kessaris N (2005). A subset of oligodendrocytes generated from radial glia in the dorsal spinal cord. *Development* 132: 1951–1959.
12. Cai J, Qi Y, Hu X, Tan M, Liu Z, Zhang J, Li Q, Sander M & Qiu M (2005). Generation of oligodendrocyte precursor cells from mouse dorsal spinal cord independent of *Nkx6* regulation and *Shh* signaling. *Neuron* 45: 41–53.
13. Richardson WD, Smith HK, Sun T, Pringle NP, Hall A & Woodruff R (2000). Oligodendrocyte lineage and the motor neuron connection. *Glia* 12, 136–142.
14. Lu QR, Yuk D, Alberta JA, Zhimin Zhu, Pawlitzky I, Chan J, McMahon AP, Stiles CD and Rowitch DH (2000). Sonic Hedgehog–Regulated Oligodendrocyte Lineage Genes Encoding bHLH Proteins in the Mammalian Central Nervous System. *Neuron* Vol. 25: 317–329.
15. Arnett HA, Fancy SPJ, Alberta JA, Zhao C, Plant SR, Kaing S, Raine CS, David H. Rowitch1, Franklin RJM and Stiles CD (2004). The bHLH transcription factor *Olig1* is required for repair of demyelinated lesions in the CNS. *Science* 306: 2111–2115.
16. Takebayashi H, Nabeshima Y, Yoshida S, Chisaka O, Ikenaka K & Nabeshima Y (2002). The basic helix–loop–helix factor *Olig2* is essential for the development of motoneuron and oligodendrocyte lineages. *Curr. Biol.* 12: 1157–1163.
17. Zhou Q & Anderson D J (2002). The bHLH transcription factors *OLIG2* and *OLIG1* couple neuronal and glial subtype specification. *Cell* 109, 61–73.
18. Dawson Mr, Levine JM and Reynolds R (2000). NG2-expressing cells in the central nervous system: are they oligodendroglial progenitors? *Journal of Neuroscience Research* 61(5):471-9.
19. Kuhlbrodt K, Herbarth B, Sock E, Hermans-Borgmeyer I and Wegner M (1998). *Sox10*, a novel transcriptional modulator in glial cells. *J Neurosci* 18: 237–250.

20. Stolt CC, Rehberg S, Ader M, Lommes P, Riethmacher D, Schachner M, Bartsch U and Wegner M (2002). Terminal differentiation of myelin-forming oligodendrocytes depends on the transcription factor Sox10. *Genes Dev* 16: 165–170.
21. Pringle NP and Richardson WD (1993). A singularity of PDGF alpha-receptor expression in the dorsoventral axis of the neural tube may define the origin of the oligodendrocyte lineage. *Development* 117: 525-533
22. Qi Y, Cai J, Wu Y, Wu R, Lee J, Fu H, Rao M, Sussel L, Rubenstein J, Qiu M (2001). Control of oligodendrocyte differentiation by the Nkx2.2 homeodomain transcription factor. *Development*. 128(14): 2723-33.
23. Aguirre A, Dupree JL, Mangin JM and Gallo VA (2007). Functional role for EGFR signalling in myelination and remyelination. *Nature Neurosci.* 10: 990–1002.
24. Armstrong RC, Kim JG and Hudson LD (1995). Expression of myelin transcription factor I (MyTI), a "zinc- finger" DNA-binding protein, in developing oligodendrocytes. *Glia* 14: 303–321.
25. Chandran, S. *et al.* (2004). FGF-dependent generation of oligodendrocytes by a hedgehog-independent pathway. *Development* 130: 6599–6609.
26. Kessaris N, Fogarty M, Iannarelli P, Grist M, Wegner M, Richardson WD (2006). Competing waves of oligodendrocytes in the forebrain and postnatal elimination of an embryonic lineage. *Nat Neurosci.* 9:173-179.
27. Nery S, Wichterle H and Fishell G (2001). Sonic hedgehog contributes to oligodendrocyte specification in the mammalian forebrain. *Development* 128: 527-540.
28. Nishiyama A (2007). Polydendrocytes: NG2 cells with many roles in development and repair of the CNS. *Neuroscientist* 13, 62–76.
29. Wilson HC, Scolding NJ, Raine CS (2006). Co-expression of PDGF alpha receptor and NG2 by oligodendrocyte precursors in human CNS and multiple sclerosis lesions. *J Neuroimmunol* 176:162–173.
30. Sommer I & Schachner M (1981). Monoclonal antibodies (O1 to O4) to oligodendrocyte cell surfaces: an immunocytological study in the central nervous system. *Dev. Biology* 83: 311-327.
31. Baron W, Shattil SJ, French-Constant C (2002). The oligodendrocyte precursor mitogen PDGF stimulates proliferation by activation of  $\alpha(v)\beta3$  integrins. *EMBO J* 21: 1957-66.
32. Fok-Seang J, Miller RH (1994). Distribution and differentiation of A2B5+ glial precursors in the developing rat spinal cord. *J Neurosci Res* 37: 219-35.
33. Hart IK, Richardson WD, Bolsover SR and Raff MC (1989). PDGF and intracellular signalling in the timing of oligodendrocyte differentiation. *Cell Biology* 109: 3411-3417
34. Raft MC, Mirsky R, Fields KL, Lisak RP, Dorfman SH, Silberberg DH, Gregson NA, Leibowitz S, and Kennedy MC (1978). Galactocerebroside is a specific cell-surface antigenic marker for oligodendrocytes in culture. *Nature* 274:813-816.
35. Dubois-Dalcq M, Behar T, Hudson L, Lazzarini RA (1986). Emergence of three myelin proteins in oligodendrocytes cultured without neurons. *J Cell Biol* 102(2):384-92.
36. Stolt CC, Rehberg S, Ader M, Lommes P, Riethmacher D, Schachner M, Bartsch U and Wegner M (2002). Terminal differentiation of myelin-forming oligodendrocytes depends on the transcription factor Sox10. *Genes Dev* 16: 165-170.
37. Nicolay DJ, Doucette JR, Nazarali AJ (2007). Transcriptional control of oligodendrogenesis. *Glia* 55: 1287-99.
38. Morell P, Quarles RH and Norton WT (1994). Myelin formation, structure and biochemistry. *Basic Neurochemistry* 117-143.
39. Franklin RJM, French-Constant C (2008). Remyelination in the CNS: from biology to therapy. *Nat. Rev. Neurosci.* 9: 839–855.

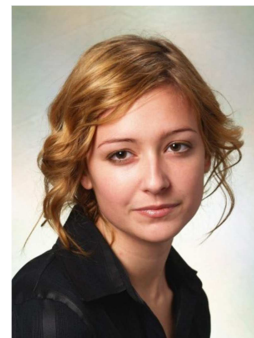
40. Bunge MB, Bunge RP and Rish H (1961). Ultrastructural study of remyelination in an experimental lesion an adult cat spinal cord. *BiophysBiochem Cytol* 10: 67-94.
41. Dawson J, Miltz W, Mir AK, Wiessner C (2003). Targeting monocyte chemoattractant protein-1 signalling in disease. *Expert Opin. Ther. Targets* 7: 35-48.
42. Watanabe M, Toyama Y, Nishiyama A (2002). Differentiation of proliferated NG2-positive glial progenitor cells in a remyelinating lesion. *J Neurosci Res* 69: 826-36.
43. Menn B, Garcia-Verdugo JM, Yaschine C, Gonzalez-Perez O, Rowitch D, Alvarez-Buylla A (2006). Origin of oligodendrocytes in the subventricular zone of the adult brain. *J Neurosci*, 26: 7907-18.
44. Zhao C, Zawadzka M, Roulois AJ, Bruce CC, Franklin RJ (2008). Promoting remyelination in multiple sclerosis by endogenous adult neural stem/precursor cells: defining cellular targets. *J Neurol Sci* 265: 12-6.
45. Smith KJ, Blakemore WF & McDonald W (1979). Central remyelination restores secure conduction. *Nature* 280, 395–396
46. Ludwin SK. (1997). The pathobiology of the oligodendrocyte. *Neuropathol Exp Neurol* 56: 111-124.
47. Blakemore WF (1974). Pattern of remyelination in the CNS. *Nature*; 249: 577-8.
48. Ludwin SK & Maitland M (1984). Long-term remyelination fails to reconstitute normal thickness of central myelin sheaths. *J Neurol Sci* 64, 193–198.
49. Stidworthy MF, Genoud S, Suter U, Mantei N & Franklin RJM(2003). Quantifying the early stages of remyelination following cuprizone-induced demyelination. *Brain Pathol.* 13, 329–339.
50. Chomiak T, Hu B (2009). What Is the Optimal Value of the g-Ratio for Myelinated Fibers in the Rat CNS? A Theoretical Approach. *PLoS ONE* 4(11): e7754.
51. Franklin RJM & ffrench-Constant C (2008). Remyelination in the CNS: from biology to therapy. *Nature Reviews Neuroscience* 9, 839-855.
52. Nave KA, Trapp BD (2008). Axon–glial signaling and the glial support of axon function. *Annu. Rev. Neurosci.* 31: 535–561.
53. Gallo V & Armstrong RC (2008). Myelin repair strategies: a cellular view. *Curr Opin Neurol* 21: 278–283.
54. Patrikios P, Stadelmann C, Kutzelnigg A, Rauschka H, Schmidbauer M, Laursen H, Sorensen S, Brück W, Lucchinetti C & Lassmann H (2006). Remyelination is extensive in a subset of multiple sclerosis patients (2006). *Brain* 129, 3165–3172
55. Sim FJ, Zhao C, Penderis J and Franklin RJM (2002). The age-related decrease in CNS remyelination efficiency is attributable to an impairment of both oligodendrocyte progenitor recruitment and differentiation. *J Neurosci* 22: 2451–2459
56. Hinks, G.L., Franklin, R.J.M. (2000). Delayed changes in growth factor gene expression during slow remyelination in the CNS of aged rats. *Mol Cell Neurosci* 16, 542–556.
57. John GR, Shankar SL, Shafit-Zagardo B, Massimi A, Lee SC, Raine CS, Brosnan CF (2002). Multiple sclerosis: re-expression of a developmental pathway that restricts oligodendrocyte maturation. *Nature Med* 8: 1115-21.
58. Kuhlmann T, Miron V, Cuo Q, Wegner C, Antel J, Bruck W (2008). Differentiation block of oligodendroglial progenitor cells as a cause for remyelination failure in chronic multiple sclerosis. *Brain* 131, 1749–1758.
59. Wolswijk G (1998). Chronic stage multiple sclerosis lesions contain a relatively quiescent population of oligodendrocyte precursor cells. *Neurosci.* 18: 601–609
60. Foote AK, Blakemore WF (2005). Inflammation stimulates remyelination in areas of chronic demyelination. *Brain* 128: 528–539.

61. Robinson S, Miller RH (1999). Contact with central nervous system myelin inhibits oligodendrocyte progenitor maturation. *Dev Biol* 216: 359–368.
62. Baer AS, Syed YA, Kang SU, Mitteregger D, Vig R, Ffrench-Constant C, Franklin RJ, Altmann F, Lubec G, Kotter MR (2009). Myelin-mediated inhibition of oligodendrocyte precursor differentiation can be overcome by pharmacological modulation of Fyn-RhoA and protein kinase C signalling. *Brain* 132: 465–81.
63. Kotter MR, Li WW, Zhao C, Franklin RJM (2006). Myelin Impairs CNS Remyelination by Inhibiting Oligodendrocyte Precursor Cell Differentiation. *Journal of Neuroscience* 26: 328–32.
64. Syed YA, Baer AS, Lubec G, Hoeger H, Widhalm G, Kotter MR (2008). Inhibition of oligodendrocyte precursor cell differentiation by myelin-associated proteins. *Neurosurg Focus* 24: E5.
65. Kotter MR, Zhao C, van Rooijen N, Franklin RJM (2005). Macrophage-depletion induced impairment of experimental CNS remyelination is associated with a reduced oligodendrocyte progenitor cell response and altered growth factor expression. *Neurobiol. Dis* 18: 166–175.
66. Kotter MR, Setzu A, Sim FJ, Van Rooijen N, Franklin RJM (2001). Macrophage depletion impairs oligodendrocyte remyelination following lysolecithin-induced demyelination. *Glia* 35: 204–12.
67. Woodruff RH, Fruttiger M, Richardson WD, Franklin RJM (2004). Platelet-derived growth factor regulates oligodendrocyte progenitor numbers in adult CNS and their response following CNS demyelination. *Mol Cell Neurosci* 25: 252–262.
68. Zhao C, Li WW, Franklin RJM (2005). Differences in the early inflammatory responses to toxin-induced demyelination are associated with the age-related decline in CNS remyelination. *Neurobiol Aging*, Sep;27(9):1298–307.
69. Blakemore WF, Gilson JM, Crang AJ (2003). The presence of astrocytes in areas of demyelination influences remyelination following transplantation of oligodendrocyte progenitors. *Exp Neurol* 184: 955–63.
70. Bieber AJ, Kerr S, Rodriguez M (2003). Efficient central nervous system remyelination requires T cells. *Ann Neurol* 53: 680–4.
71. Levine JM, Reynolds R (1999). Activation and proliferation of endogenous oligodendrocyte precursor cells during ethidium bromide-induced demyelination. *Exp. Neurol* 160: 333–347.
72. Davis S, Gale NW, Aldrich TH, Maisonpierre PC, Lhotak V, Pawson T, Goldfarb M, Yancopoulos GD (1994). Ligands for EPH-related receptor tyrosine kinases that require membrane attachment or clustering for activity. *Science*, 266: 816–9.
73. Holland SJ, Gale NW, Mbamalu G, Yancopoulos GD, Henkemeyer M, Pawson T (1996). Bidirectional signalling through the EPH-family receptor Nuk and its transmembrane ligands. *Nature*, 383: 722–5.
74. Pasquale EB (1997). The Eph family of receptors. *Curr Opin Cell Biol* 9: 608–615.
75. Miranda JD, White LA, Marcillo AE, Willson CA, Jagid J, Whittemore SR (1999). Induction of Eph B3 after Spinal Cord Injury. *Experimental Neurology*, 156: 218–22.
76. Willson CA, Irizarry-Ramirez M, Gaskins HE, Cruz-Orengo L, Figueroa JD, Whittemore SR, Miranda JD (2002). Upregulation of EphA receptor expression in the injured adult rat spinal cord. *Cell Transplant*, 11: 229–39.
77. Benson MD, Romero MI, Lush ME, Lu QR, Henkemeyer M, Parada LF (2005). Ephrin-B3 is an amyelin-based inhibitor of neurite outgrowth. *Proc Natl Acad Sci U S A*, 102: 10694–9.
78. Syed Y (2010), unpublished data.
79. McMorris FA, Smith TM, DeSalvo S and Furlanetto RW (1986). IGF-I/somatomedin-C: a potent inducer of oligodendrocyte development. *Proc Natl. Acad Sci USA* 83, 822–826.
80. McMorris FA & Dubois-Dalcq M (1988). Insulin-like growth factor I promotes cell proliferation and oligodendroglial commitment in rat glial progenitor cells developing in vitro. *J Neurosci Res* 21, 199–209.

81. Flanagan JG, Vanderhaeghen P (1998). The ephrins and Eph receptors inneural development. *Annu Rev Neurosci*, 21:309-345.
82. Buckinx R, Smolders I, SahebAli S, Janssen D, Smets I, Ameloot M and Jean-Michel Rigo (2009). Morphological changes do not reflect biochemical and functional differentiation in OLN-93 oligodendroglial cells. *Journal of Neuroscience Methods*, Volume 184;1:1-9.
83. Krämer EM, Koch T, Niehaus A, Trotter J (1997). Oligodendrocytes direct glycosyl phosphatidylinositol-anchored proteins to the myelin sheath in glycosphingolipid-rich complexes. *J Biol Chem* 4;272(14):8937-45.
84. Mathisen PM, Pease S, Garvey J, Hood L & Readhead C (1993). Identification of an embryonic isoform of myelin basic protein that is expressed widely in the mouse embryo. *Neurobiology* 90:10125-10129.
85. Chen Y, Balasubramaniyan V, Peng J, Hurlock EC, Tallquist M, Li J & Lu QR (2007). Isolation and culture of rat and mouse oligodendrocyte precursor cells. *Nature Protocols* 2, 1044-1051 | doi:10.1038/nprot.2007.149.
86. Norton WT, Poduslo SE (1973): Myelination in rat brain: changes in myelin composition during brain maturation. *J Neurochem* 21(4), 759-73.
87. Trotter J, Schachner M (1989). Cells positive for the O4 surface antigen isolated by cell sorting are able to differentiate into astrocytes or oligodendrocytes. *Brain Res Dev Brain Res*. Mar 1;46(1):115-22.
88. Jung M, Kramer E, Grzenkowski M, Tang K, Blakemore W, Aguzzi A, Khazaie K, Chlichlia K, von Blankenfeld G, Kettenmann H, et al (1995) Lines of murine oligodendroglial precursor cells immortalized by an activated neu tyrosine kinase show distinct degrees of interaction with axons in vitro and in vivo. *Eur J Neurosci* 7:1245–1265.
89. Richter-Landsberg C, Heinrich M (1996). OLN-93: a new permanent oligodendroglia cell line derived from primary rat brain glial cultures. *J Neurosci Res*. Jul 15;45(2):161-73.
90. Nakada M, Drake KL, Nakada S, Niska JA & Berens ME (2006). Ephrin-B3 Ligand Promotes Glioma Invasion through Activation of Rac1. *Cancer Res* 66:8492-8500

## 8. Appendix

### 8.1 CURRICULUM VITAE



#### Details

---

Name: Tamara Weiss  
Adress: 1070 Vienna, Austria  
Academic degree: 03/2011 Bachelor of Science (University of Vienna)

#### Education

---

10/2005 – 04/2011 Study of *Molecular Biology* at the University of Vienna, Austria  
09/2000 – 06/2005 Bundeshandelsakademie Wiener Neustadt, Austria  
09/1996 – 06/2000 Bundesrealgymnasium Wiener Neustadt, Austria

#### Rotations/dissertation

---

01.03. – 31.09.2010 Degree dissertation: **'Modulating EphrinB3-signalling to enhance CNS remyelination'**,  
*Kotter Group, Anne McLaren Laboratory for Regenerative Medicine* - Department of Clinical  
Neurosciences, University of Cambridge, United Kingdom

03.08. – 30.09.2009 Rotation: **'Signal transduction & Differentiation of Cardiomyocytes'**  
*Weizer Group, Max F. Perutz Laboratories* - Department of Membranes & Cytoskeleton,  
University of Vienna, Austria

16.03. – 17.04.2009 Rotation: **'Determination of the CspA cold box binding conditions'**  
*Konrat Group, Max F. Perutz Laboratories* - Department of Biomolecular Structural Chemistry,  
University of Vienna, Austria

27.10. – 26.11.2008 Rotation: **'Structure determination of human Telomerase RNA in vitro'**  
*Waldsich Group, Max F. Perutz Laboratories* - Department of Biochemistry, University of Vienna,  
Austria

21.07. – 05.09.2008 &  
01.07. – 30.08.2007 **'betaGTase'**  
*Silke Duglai-Esser Laboratory, WACKER Chemie AG, Munich, Germany*

#### Scholarships

---

2010 *'Förderstipendium der Universität Wien'*

2010 *'Leistungsstipendium der Universität Wien' (05.10.2009 - 23.10.2009)*

2010 *'NÖ Top-Stipendium Ausland'*

### Employments

---

03/2011 – 06/2011	Tutor position at the University of Vienna, Austria
10/2010 – 02/2011	Tutor position at the University of Vienna, Austria
10/2009 – 02/2010	Tutor position at the University of Vienna, Austria
04/2003 – 06/2006	part-time job (consulting, sales, calculations) <i>J. M. Reger Rahmenstudio</i> , Austria, Wiener Neustadt

### Further Education (Courses, Seminars, Symposia)

---

29. – 31.03.2010	<i>Spring School 2009</i> , Cambridge Centre for Brain Repair, Cambridge, UK Topics of Neurosciences
13. – 15.01.2009	<i>EMBO Workshop</i> , Austria, Vienna Regulatory RNAs in Pro- & Eucaryotes
17. – 18.07.2007	<i>IBA-Academy</i> , Germany, Munich Seminar: ‘advanced protein chemistry’
01. – 09.07.2004	6 <sup>th</sup> <i>summer academy for highly skilled students</i> , Austria Course: biology/chemistry

### Further skills

---

IT knowledge	Very good knowledge of <i>MS Word</i> , <i>MS PowerPoint</i> and <i>Macromedia Fireworks MX</i> (image editing). <i>Microsoft Excel</i> (basic) <i>Vektor NTI</i> (basic) <i>ImageJ</i> (basic)
Foreign language	English (good)

---

Date

Signature